



DURBAN UNIVERSITY OF TECHNOLOGY
INYUVESI YASETHEKWINI YEZOBUCHWEPHESHE

**PERFORMANCE ANALYSIS OF FILTERED
ORTHOGONAL FREQUENCY DIVISION
MULTIPLEXED LDPC CODES FOR SATELLITE
COMMUNICATION IN THE KA-BAND**

by

Bonginkosi Gumede

Student Number: 20302473

**Thesis submitted in compliance with the requirements for the
Master of Engineering Degree.**

**DEPARTMENT OF ELECTRONIC AND COMPUTER
ENGINEERING
FACULTY OF ENGINEERING AND THE BUILT
ENVIRONMENT**

DECLARATION

I declare that this thesis represents my own work and has not been previously submitted to any other university for any degree. All information cited from published work has been acknowledged.

Approved for Final Submission

Student



27/11/2023

Mr B Gumede

Date

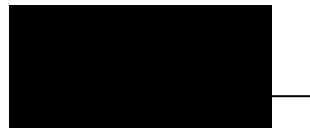
Supervisor



13 March 2024

Dr E Mukubwa

Date



13/03/2024

Date

ACKNOWLEDGEMENTS

I sincerely thank God for granting me the strength, good health, knowledge, and empowerment to persevere. Without his divine presence, none of this would have been achievable. I would like to express my heartfelt appreciation to my supervisors, Dr. E. Mukubwa and Dr. N Pillay, for their unwavering dedication in supporting me throughout my research journey. His guidance, knowledge, and encouragement have been instrumental in helping me reach new heights and achieve my aspirations. I am also grateful to Prof. Davidson for his ongoing support and guidance in this endeavor. I extend great appreciation to my wife, Sharon, for her unwavering support, love, encouragement, and patience throughout the early mornings and long hours I devoted to completing this research. Having her by my side is truly a blessing, and I wouldn't have made it without her support.

I am forever grateful to my late father, Simon Gumede, and my late mother, Fikelephi Gumede, for their unwavering support in my career pursuits. Their belief in me has consistently motivated me. Lastly, I would also like to convey my gratitude to my children, Buhle and Bahle, for bringing happiness and joy into my life, particularly when I needed them the most.

Bonginkosi Gumede

ABSTRACT

The saturation of lower frequency bands and the growing demand for high data rates have presented the need to design future systems at Ka-band frequency, but Ka-band frequency is very fragile because of the millimeter wavelength. Ka-band frequencies range from 26 to 40 GHz, making the signal more susceptible to weather impairments and shadowing than lower frequency bands. Rain attenuation is a major problem in satellite communications systems operating at Ka-band, it causes major signal degradation because the raindrop is about the size of the Ka-band wavelength. To mitigate this problem, you must use powerful Forward Error Correction (FEC) codes such as Low Density Parity Check (LDPC) or Turbo codes. This research presents the performance of LDPC codes for satellite communications in the Ka-band, we enhance the system's performance by adding adaptive modulation and filtered - Orthogonal Frequency Division Multiplexing (f-OFDM).

This research study has been undertaken as follows: First, we studied the operation of LDPC codes, including different encoding and decoding techniques. We decided to use the Quasi Cyclic (QC) parity check matrix, allowing us to employ the QC-LDPC encoding technique, which reduces encoding complexity and improves coding efficiency. We explored various LDPC code decoding techniques and opted for soft decoding techniques, namely Belief Propagation, Layered Belief, Normalised Min-Sum, and Offset-Min Sum, as they are more effective in reducing errors compared to hard decision decoding. The Ka-band satellite channel is modeled using the Gaussian distribution, considering that the signal envelope and signal phase change randomly after passing through the Ka-band channel. All parameters were set according to different weather conditions. For the simulations, we utilized the MATLAB software package.

The uncoded 16-Quadrature Amplitude Modulation (QAM) OFDM system on moderate rain weather conditions achieved a gain of 4.3 dB against light snow and thunderstorm weather conditions at the BER 10^{-3} . We applied f-OFDM, and the results show that LDPC codes achieve a gain of 2 dB when compared to Turbo codes and a gain of 3 dB compared to Convolutional Codes (CC) at the BER of 10^{-3} under moderate rain conditions in the Ka-band channel, we can see the effects of f-OFDM and LDPC codes. When adding the adaptive modulation into the system, modulation switches from 16-

QAM to 64-QAM at E_b/N_0 of -9 dB and switches from 64-QAM to 256-QAM at E_b/N_0 of -5 dB thus improving spectral efficiency. The system is resilient and feasible in error correction at low Signal to Noise Ratio (SNR).

Table of Contents

ACKNOWLEDGEMENTS.....	II
ABSTRACT.....	III
Table of Contents	5
List of Figures	8
List of Tables.....	9
CHAPTER ONE.....	10
General Introduction.....	10
1.1 Introduction	10
1.2 Problem Statement.....	11
1.3 Study Objectives.....	12
1.4 Methodology	13
1.4.1 Simulation Tool	13
1.5 Contributions	14
1.6 Motivation	14
1.7 Outline of the Dissertation	15
1.8 Summary	16
1.9 Publications Emanating from this Thesis	18
CHAPTER TWO.....	19
The Literature Review of LDPC Codes, f-OFDM, Adaptive Modulation, and Ka-band Frequency	19
2.1 LDPC Codes.....	19
2.2 LDPC Encoding.....	20
2.3 Decoding of LDPC Codes	23
2.3.1 Soft Decision Decoding.....	24
2.3.2 Hard Decision Decoding.....	30
2.4 Adaptive Modulation	32
2.4.1 Early Developments	32

2.4.2 Advancements in Adaptive Modulation.....	32
2.4.3 Adaptive Modulation in MIMO Systems.....	33
2.4.4 Recent Advances and Energy Efficiency	33
2.4.5 Adaptive Modulation and Coding for NTN Network.....	36
2.5 Orthogonal Frequency Division Multiplexing.....	37
2.5.1 FFT and IFFT	37
2.6 The f-OFDM system.....	38
2.7 Ka-band Satellite Channel Model	39
2.8 Integration of LDPC codes, OFDM, f-OFDM, and Adaptive Modulation	42
2.9 Summary	43
CHAPTER THREE.....	44
Modeling and Design of the System	44
3.1 Introduction	44
3.2 The System Model.....	44
3.2.1 LDPC Codes.....	44
3.2.2 Adaptive Modulation.....	55
3.2.3 The f-OFDM	55
3.2.4 The Channel Model	56
3.2.5 The working of the system.....	59
3.2.6 The Summary	62
CHAPTER FOUR	64
Simulations and Results Discussion.....	64
4.1 Introduction	64
4.2 The System Simulation	64
4.2.1 LDPC Code Parameters.....	64
4.2.2 LDPC Encoder and Decoders	64
4.2.3 Modulator and OFDM Parameters.....	65
4.2.3 Channel Parameters:	65

4.2.4 Simulation Stopping Criteria:	66
4.1 Matlab Simulation Parameters	66
4.2 Results Discussion.....	67
CHAPTER FIVE.....	75
Conclusion and Recommendations	75
5.1 Conclusion.....	75
5.2 Recommendations	77
REFERENCES.....	78

List of Figures

Figure 3 - 1: Tanner graph of parity check matrix H	46
Figure 3 - 2: The statistical immovable Ka-band satellite communication model [4]......	58
Figure 3 - 3: Block diagram of the system with LDPC codes, adaptive modulation, f-OFDM and the fixed Ka-band channel model.....	61
Figure 3 - 4: Block diagram of the system with LDPC codes, adaptive modulation, f-OFDM, LMS and the Fixed Ka-Band Satellite Channel.....	61
Figure 4 - 1: Uncoded 16-QAM - OFDM under all Ka-band weather scenarios	68
Figure 4 - 2: 16-QAM - OFDM LDPC coded under all Ka-band weather scenarios	68
Figure 4 - 3: Uncoded 16-QAM-OFDM vs LDPC coded 16-QAM-OFDM.....	68
Figure 4 - 4: LDPC coded 16-QAM f-OFDM vs LDPC coded 16-QAM OFDM on moderate rain in the Ka-band satellite channel.....	69
Figure 4 - 5: LDPC code 16-QAM f-OFDM vs Turbo code 16-QAM f-OFDM vs CC 16-QAM f-OFDM on moderate rain weather in the Ka-band satellite channel.....	70
Figure 4 - 6: Simulation of different M-QAM levels.....	71
Figure 4 - 7: Comparison of LDPC decoding iterations 3, 5, and 10.....	72
Figure 4 - 8: LDPC soft decoding algorithms comparison.....	72
Figure 4 - 9: LDPC codes QAM f-OFDM adaptive modulation: Ka-band satellite channel on moderate weather.....	73
Figure 4 - 10: Spectral efficiency of LDPC codes QAM f-OFDM adaptive modulation: Ka-band satellite channel on moderate weather.	74

List of Tables

Table 2 - 1: Overview of messages received and sent by the check nodes.....	31
Table 2 - 2: Message node decisions for hard decision decoder.	31
Table 2 - 3: Parameter Adaptation Thresholds	35
Table 2 - 4: Modulation order and BER thresholds	35
Table 3 - 1: Immovable Ka-band satellite weather envelope attenuation measurements.	58
Table 3 - 2: Immovable Ka-band satellite weather phase attenuation measurements.	58
Table 3 - 1 Switching threshold for M-QAM SNR-based adaptive modulation algorithm...58	
Table 4 - 1: LDPC Parameters.....	66
Table 4 - 2: Modulator and OFDM Parameters.....	66
Table 4 - 3: Channel Parameters.....	67

CHAPTER ONE

General Introduction

1.1 Introduction

The field of telecommunications is undergoing rapid transformation with the increasing demand for high-speed data services. The transition from the Fourth-Generation (4G) Mobile Networks to Fifth Generation (5G) Mobile Networks has already taken place, and the prospect of the Sixth Generation (6G) Mobile Networks, also known as beyond 5G, is on the horizon. The 6G networks are anticipated to integrate terrestrial mobile networks with satellite networks, scheduled for introduction around the year 2030 [1]. To ensure the success of these ambitious 6G networks, satellite systems must provide reliable high data rates. However, the saturation of low-frequency bands like the L-band has compelled designers to explore higher-frequency bands, particularly the Ka-band, due to its vast available spectrum. The Ka-band offers exciting opportunities, including a greater number of channels, high data rate services, and the option to trade bandwidth for implementation simplicity [2].

Although the Ka-band presents promising possibilities, it also poses significant challenges due to its high-frequency nature. These challenges include channel impairments such as attenuation, fading, and interference, which can adversely affect the performance of satellite communication systems operating in this frequency range [3] - [4]. Researchers have sought to address these issues by utilizing powerful Forward Error Correction (FEC) codes like Low-Density Parity Check (LDPC) codes [3]. While LDPC codes have proven effective in combating the effects of rain attenuation in the Ka-band satellite communication, some studies have revealed that their full potential remains untapped [4].

Existing systems employing LDPC codes with fixed modulation schemes, such as Binary Phase Shift Key (BPSK) and QAM, exhibit limited data rates, poor spectral efficiency, and susceptibility to interference, ultimately leading to suboptimal system performance. To overcome these limitations, this study proposes the incorporation of adaptive modulation and filtered Orthogonal Frequency Division Multiplexing (f-OFDM) into the satellite Ka-band communication system. The integration of adaptive modulation and f-OFDM aims to enhance the robustness of LDPC codes and mitigate the effects of rain fade effectively. By combining these advanced techniques, the research aims to unleash the full capability of LDPC codes

and explore the potential of the Ka-band for high data rate transmissions with reduced Bit Error Rate (BER).

1.2 Problem Statement

The evolution of mobile and fixed networks is happening at a fast rate due to a growing demand for broadband data services. We are currently on 5G mobile communication networks. The next generation of mobile networks, 6G, is expected to integrate terrestrial mobile networks with satellite networks [1], it is expected to be introduced by the year 2030, therefore, satellite systems must provide reliable high data rates. On the other hand, the saturation of low-frequency bands such as the L-band and other bands has caused a shift to designing satellite systems in the Ka-band. The advantage of the Ka-band is the amount of available spectrum. Ka-band offers these opportunities [2]:

- A greater number of channels.
- High data rate services.
- Bandwidth can be sacrificed for simplicity of implementation.

The high frequency of Ka-band signals poses significant challenges, including channel impairments such as attenuation, fading, and interference [3]-[4]. Based on the above-mentioned Ka-band problems, it is vital to design a satellite Ka-band system that will be able to reduce BER by using powerful FEC codes, such as LDPC codes. Researchers in [3] have used LDPC codes to overcome the rain attenuation in the Ka-band satellite communication, but their system used fixed BPSK and QAM schemes, which have poor spectral efficiency, limited data rates, and are susceptible to interference. These limitations lead to poor system performance, meaning that even if you are using LDPC codes, you still do not explore the full capability of the system. To overcome these problems, we propose adding adaptive modulation and f-OFDM into the system.

To delimit the field being investigated, this study focuses specifically on the integration of LDPC codes with adaptive modulation and f-OFDM in the Ka-band satellite communication systems. This delimitation is essential to narrow the scope of the research and provide a focused investigation into the specific techniques that can enhance the performance of Ka-band satellite communication systems. By concentrating on the integration of LDPC codes with adaptive modulation and f-OFDM, the study aims to address the specific challenges

posed by rain attenuation in the Ka-band satellite communication, offering targeted solutions to optimize system performance under these conditions. This focused approach enables a comprehensive analysis of the effectiveness of these integrated techniques in mitigating rain attenuation and improving the reliability and efficiency of Ka-band satellite communication systems.

1.3 Study Objectives

This work investigates the performance of LDPC codes in the Ka-band. It is necessary to study the fundamentals of LDPC codes and study the Ka-band properties. This allows us to formulate the models to be used in this study, the main goal is to mitigate the effects of rain fade in the Ka-band by using LDPC codes, adaptive modulation, and f-OFDM. The overall study is arranged into the following research objectives:

- Investigate LDPC codes, Ka-band satellite channel model, f-OFDM, and adaptive modulation.
- Implement the combination of LDPC codes, Ka-band, f-OFDM, and adaptive modulation in MATLAB.
- Compare and evaluate the simulation results of LDPC codes, f-OFDM, and adaptive modulation system to Turbo codes and Convolutional Codes (CC) to prove the robustness of the system in mitigating the rain fade in the Ka-band satellite channel.

The above research objectives can be broken down into the following research questions:

- Research Question 1: How does a combination of LDPC codes, f-OFDM, and adaptive modulation work?
- Research Question 2: How can a combination of LDPC codes, f-OFDM, and adaptive modulation be implemented in a Ka-band satellite channel model?
- Research Question 3: What specific enhancements can be identified through the comparison and evaluation of LDPC codes to Turbo codes and CC when applying f-OFDM and adaptive modulation systems to all three FEC codes in simulated scenarios aimed at demonstrating the robustness of LDPC codes in effectively mitigating rain fade within the Ka-band satellite channel?

The following sub-section describes the methods used to achieve the above-mentioned objectives.

1.4 Methodology

The study of LDPC codes in combating noise at low Signal to Noise Ratio (SNR) is gaining momentum across all fields of digital communications because of the powerful nature of LDPC codes. On the other hand, there is a move to design systems at Ka-band because of spectrum limitations at low-frequency bands. The work of this thesis relied upon previous related studies, which established the foundation. We significantly improved upon this foundation by implementing f-OFDM and adaptive modulation. This allowed us to address the research question of mitigating rain fade in the Ka-band. We approached the research by conducting a preliminary study of LDPC codes. We looked at the trends, models, challenges, and benefits of this study. We then conduct the literature study of the research problem. The literature review provides guidance and in-depth insight into what is expected in terms of the research input and output. In the literature, we studied previous papers and journals on LDPC codes, OFDM, f-OFDM, Additive White Gaussian Noise (AWGN) channel model, the Ka-band channel model, and adaptive modulation. Each component of the system model is studied separately and later combined to form the system model.

1.4.1 Simulation Tool

The simulation software chosen for this research is MATLAB because it can offer the following benefits:

- MATLAB has a very strong mathematical calculation ability compared to Python.
- MATLAB has special toolboxes for communications, signal processing, 5G, Wireless Local Area Networks (WLAN), and many others.
- Database of built-in algorithms and functions.
- Easy to run simulations and debugging.

The LDPC Parity Check Matrix, LDPC encoder, modulator, channels, demodulator, and decoder functions are complicated and time-consuming when formulating a code, but MATLAB allows you to use some of the built-in functions that reduce the code length. We decided on the results based on the BER, simulations were conducted repeatedly and compared to find the best results.

1.5 Contributions

There have been contributions made by previous work related to this study, they also focused on mitigating Ka-band weather effects by using LDPC codes. The main contribution of this work is to use LDPC codes with adaptive modulation and f-OFDM in mitigating Ka-band weather effects problems. Preliminary simulations have proven the effectiveness of this combination when comparing the results of LDPC codes, adaptive modulation, and f-OFDM by comparing them to Turbo codes and CC. The contributions of this research can be summarized as follows:

- LDPC codes have been proven to be effective and feasible in error correction at the Ka-band satellite channel.
- LDPC codes with f-OFDM and adaptive modulation have proven to be more effective in error correction at the Ka-band satellite channel.
- It has been proven that the Ka-band is suitable for high data rate transmission with low BER when using LDPC codes with adaptive modulation and f-OFDM.
- Reduction of LDPC code processing time by using simple but effective encoding algorithms and decoding algorithms, thus reducing the computing time.

1.6 Motivation

The Ka-band has become attractive for future satellite system design because low bands are becoming saturated, therefore this has presented a need for studies such as this one. Higher frequencies are very fragile because of the nature of short wavelengths not being able to penetrate surfaces easily. The motivation for using LDPC codes to mitigate the effects of weather impairments, such as rain attenuation, in the Ka-band channel comes from numerous recent studies that demonstrate the robustness of LDPC codes. The basic idea is to ensure that we reduce computing time when designing LDPC codes because the satellite channel has

already presented a latency problem, therefore, we must use a simple encoding and decoding structure. The study has been motivated by the research study [3], which has proven the robustness and effectiveness of LDPC codes in reducing BER in the Ka-band satellite systems. They presented the design of LDPC codes, including decoding and encoding. Different schemes of modulation and demodulation were used with LDPC codes showing good simulation results however; they did not use adaptive modulation and f-OFDM. The advantages of adaptive modulation are as follows:

- Increased data throughput on favourable channel conditions
- Maintain the radio link on worst channel conditions with reduced data.
- Increased flexibility of the system.
- Improved spectral efficiency.

Therefore, it is necessary to implement adaptive modulation as part of this study based on the above-mentioned advantages.

1.7 Outline of the Dissertation

The research study titled "Performance Analysis of Filtered Orthogonal Frequency Division Multiplexed LDPC Codes for Satellite Communication in the Ka-Band" requires an understanding of digital telecommunication fundamentals to model and design the system. LDPC codes, OFDM, f-OFDM, adaptive modulation, and the Ka-band channel are the building blocks of the system, making it crucial to comprehend and mathematically analyse each block. Mathematical analysis was employed to model the system, which was then implemented in Matlab for simulations and testing. The thesis is organized as follows: Chapter 2 presents the literature review of LDPC codes, f-OFDM, adaptive modulation, and Ka-band channel. Chapter 3 focuses on the system's modeling and design, detailing the research methodology, theoretical study, mathematical algorithms, analysis, and system models. Chapter 4 provides the research results and analysis, while Chapter 5 offers the conclusion and recommendations for future studies.

1.8 Summary

The evolution of mobile and fixed networks has been driven by the soaring demand for broadband data services, resulting in the development and deployment of 5G mobile communication networks. Looking towards the future, the prospects of the sixth-generation mobile networks, termed beyond 5G, are approaching, necessitating the integration of terrestrial mobile networks with satellite networks. Expected to be introduced around 2030, these 6G networks require satellite systems capable of providing reliable high data rates.

The shift to higher-frequency bands, particularly the Ka-band, has been prompted by the saturation of low-frequency bands like the L-band. Ka-band's abundance of available spectrum has made it an attractive choice for satellite systems, offering numerous advantages, including a greater number of channels, high data rate services, and the potential for simpler implementation by trading bandwidth. However, the Ka-band's high-frequency nature presents significant challenges, including attenuation, fading, and interference, which can adversely affect satellite communication performance. In an effort to combat these issues, researchers have turned to powerful FEC codes such as LDPC codes. While LDPC codes have shown promise in addressing rain attenuation in the Ka-band satellite communication, previous systems utilizing LDPC codes with fixed modulation schemes have exhibited limited data rates, poor spectral efficiency, and susceptibility to interference, leading to suboptimal performance.

This study proposes a comprehensive approach to improve the performance of Ka-band satellite communication systems by integrating adaptive modulation and f-OFDM with LDPC codes. By doing so, the research aims to enhance the robustness of LDPC codes, overcome the limitations of fixed modulation schemes, and effectively mitigate rain fade in the Ka-band. The combined use of these advanced techniques seeks to unlock the full potential of LDPC codes and exploit the capabilities of the Ka-band for high data rate transmissions with low BER. To achieve these objectives, the study outlines a series of research questions and objectives, including an investigation of LDPC codes, Ka-band satellite channel model, f-OFDM, and adaptive modulation. The implementation of these techniques in MATLAB is explored, and simulation results are compared to Turbo codes and CC to demonstrate the robustness of the proposed system in mitigating rain fade in the Ka-band satellite channel.

The study's methodology involves a thorough literature review of LDPC codes, OFDM, f-OFDM, AWGN channel model, Ka-band channel model, and adaptive modulation. The various components of the system model are studied independently before being integrated into a comprehensive system model. Contributions of this research include the demonstration of the effectiveness and feasibility of LDPC codes for error correction in the Ka-band satellite channel. Moreover, the combination of LDPC codes with adaptive modulation and f-OFDM has been shown to enhance error correction capabilities further, making the Ka-band suitable for high data rate transmissions with low BER. Additionally, the study focuses on reducing LDPC code processing time by employing simple yet effective encoding and decoding algorithms.

The motivation for this study arises from the need to design future satellite systems at the Ka-band due to the saturation of lower frequency bands. Given the fragility of higher frequencies, especially in the face of rain attenuation, the use of LDPC codes to combat weather effects in the Ka-band is well-founded. The research aims to reduce computing time by adapting a straightforward encoding and decoding structure for LDPC codes, essential for addressing latency issues in the satellite channel. The work builds upon previous studies that have demonstrated the robustness of LDPC codes in reducing BER in the Ka-band satellite systems.

The dissertation is structured to provide an overview and literature review of LDPC codes, f-OFDM, adaptive modulation, and Ka-band channel, followed by a detailed description of the system's modeling and design. Simulation results and analysis are presented, leading to the conclusion and recommendations for future studies. The research's significance lies in its potential to enhance satellite communication performance in the Ka-band, thereby contributing to the advancement of future 6G networks and meeting the growing demand for high-speed data transmission.

1.9 Publications Emanating from this Thesis

The following is a technical publication emanating from this thesis:

Bonginkosi Gumede, Emmanuel Mukubwa, Nelendran Pillay and Innocent E Davidson, “Performance Analysis of Filtered Orthogonal Frequency Division Multiplexed LDPC Codes for Satellite Communication in the Ka-Band”, in AFRICON 2023 IEEE proceedings. Paper presented at the IEEE Africon Conference, Sep 20 – 22, 2023, Kenya School of Monetary Studies, Nairobi, Kenya.

CHAPTER TWO

The Literature Review of LDPC Codes, f-OFDM, Adaptive Modulation, and Ka-band Frequency

2.1 LDPC Codes

LDPC codes are a class of linear error-correcting codes known for their excellent error-correction capabilities and efficient decoding algorithms. They were introduced by Gallager in 1962 [5], but their full potential was realized much later due to the discovery of efficient iterative decoding algorithms, such as the belief propagation algorithm. LDPC codes are characterized by sparse parity-check matrices, typically denoted by H , which determine the relationships between the input data bits and the parity-check bits. The sparsity of H is one of the reasons for the efficient decoding of LDPC codes. The elements of H are usually binary, with 1 representing a non-zero coefficient and 0 representing no connection between a data bit and a parity-check bit. The encoding and decoding processes of LDPC codes can be described using matrix operations. Let x be the vector of input data bits of length k , and c be the vector of codeword bits of length n . The encoding

$$c = x * G \tag{2.1}$$

where G is the generator matrix of the LDPC code, which is usually constructed using sparse matrices to preserve the sparsity properties of LDPC codes [5].

Decoding LDPC codes can be done using iterative algorithms, the most common being the Belief Propagation (BP) algorithm, also known as the sum-product algorithm. The BP algorithm uses message passing between variable nodes and check nodes of the code's Tanner graph to iteratively update the probabilities of the codeword bits being 0 or 1 [6]. One of the first practical applications of LDPC codes was in the field of digital communication, where they were adopted for error correction in various communication systems. Their performance was found to be close to the Shannon limit, making them highly attractive for modern communication standards, such as Wi-Fi, WiMAX, and DVB-S2 [7]. LDPC codes have also found applications beyond communication systems. They have been used in storage systems, such as hard drives and flash memory, to enhance data reliability [8]. Additionally, LDPC codes have been explored in the context of quantum error correction, where they show promise for efficiently correcting errors in quantum information processing [9]. LDPC codes are an important class of error-correcting codes with remarkable error-correction capabilities

and efficient decoding algorithms. They have been successfully applied in various communication and storage systems and continue to be a subject of research interest in both classical and quantum information processing.

2.2 LDPC Encoding

The LDPC encoder is an essential component in the communication system because it generates LDPC codewords from the incoming information bits [10]. The encoding process of an LDPC code involves the mapping of information bits to codewords using a parity-check matrix [11]. The design of this matrix is a critical factor that determines the performance of an LDPC code [12] and the design of efficient LDPC encoding techniques is a critical research area that has gained significant attention in recent years. These techniques aim to improve the throughput and encoding complexity of LDPC codes, making them suitable for high-performance communication systems.

Several techniques have been proposed to improve the encoding performances of LDPC codes. One such technique is using a mixed-radix approach that reduces the encoding complexity of large-sized LDPC codes [13]. Another proposed technique is the use of layered encoding which improves the encoding throughput [14]. In recent years, many researchers have explored the use of hardware-based LDPC encoders to achieve high-throughput encoding [15]. Several implementations of LDPC encoders using Field-Programmable Gate Arrays (FPGAs) have been proposed [16]. These hardware-based LDPC encoders provide high-speed encoding capabilities, making them ideal for use in high-performance communication systems.

The most popular approach for designing LDPC matrices is using the Tanner graph representation [17]. Tanner graph-based LDPC encoder proposed by Chen et al. [17] utilizes a modified quasi-cyclic structure that results in a more efficient implementation with lower computational complexity. Another notable LDPC encoder is the Layered Belief Propagation (L-BP) encoder introduced by Hu et al. in [18]. This encoder utilizes layered decoding iteratively and sequentially to improve the encoding speed while achieving performance similar to that of other LDPC encoders. Gulak et al. published their research work in [19] proposing a novel LDPC encoder based on a tree structure, which significantly reduces the implementation complexity by eliminating the need for a full parity check matrix. The

proposed encoder achieved competitive performance while reducing the gate count and power consumption. Recently, a new type of LDPC encoder called the graph decomposition low-density parity check (GD-LDPC) encoder, introduced by Xu et al. in [20]. This encoder decomposes the original parity check matrix into several smaller parity check matrices, which reduces the implementation complexity and improves the encoding speed while maintaining the same error correction performance. Different LDPC encoders have been proposed with varying implementation structures, complexities, and performance by Chen et al. [17], Hu et al. [18], Gulak et al. [19], and Xu et al. [20] proposed different implementations for LDPC encoders, each with its advantages and limitations. These developments pave the way for the practical application of LDPC codes in various communication and storage systems.

We have seen above that there are different types of LDPC encoding techniques, but the general form of encoding is as follows, say we have information bits k which form the data word s , information bits k are the same as s bits, but we prefer to call it data word s . LDPC coded word is called c codeword as defined in eqn 2.1, it is made of k information bits of data word s and m parity check bits. The length of codeword c can be expressed as n , where $n = k + m$. Decoding becomes easy because at the decoder, we simply extract k bits from the decoded word c' to obtain data word s' Linear encoding is as follows:

$$G \cdot H^T = 0, \quad (2.2)$$

where G is a generator matrix, please see equation 2.1.

$$c = G^T \cdot s \quad (2.3)$$

This works well for codes such as hamming codes but not for LDPC codes because H can be very large, and it is a sparse matrix that may not generate a good sparse generator matrix G . This leads to encoding complexity which increases the computing time. The solution is to use Repeat Accumulate (RA)-LDPC codes [21] or the Quasi-Cyclic (QC)-LDPC encoder for IEEE 802.11n which has reduced encoding complexity [22]. The encoding is fast, it does not overload the processors. The RA-LDPC encoder operation is presented in algorithm 2.1 and the QC-LDPC encoder operation is presented in algorithm 2.2. RA-LDPC parity check matrix H is made of two submatrices which are H_s (parity check matrix which controls source bits) and H_p (parity check matrix which controls parity bits). The QC-LDPC encoder presented in [22] is based on Richardson and Urbanke lower-triangular algorithm for IEEE 802.11n wireless LAN standard for 648 block length and the code rate of 1/2. There is a choice to use codeword length blocks of 129 and 1944 for a total of 12 possible codes and the information

rate can be varied depending on the choice of an encoder designer. This encoder is less complex and compatible with high-speed applications; hence, we selected this encoder for implementation in this study. This encoder is designed by converting the base matrix into the lower triangular matrix approximation by dividing the matrix into submatrices A, B, C, D, T , and E [22]. Simplified encoding steps are shown in algorithm 2.2.

Algorithm 2.1 Repeat Accumulate LDPC encoding.

Input data: s - data, $H = [H_s H_p]$ - parity check matrix of RA-LDPC

Output data: $c = [s p]$ - codeword

Step 1: Compute $v = H_s s$

Step 2: Compute parity bits p as follows

$$\begin{aligned}
 p_1 &= \sum_{i=1}^k H_{s1i} S_i = v_1 \\
 p_2 &= p_1 + \sum_{i=1}^k H_{s2i} S_i = p_1 + v_2 \\
 p_3 &= p_2 + \sum_{i=1}^k H_{s3i} S_i = p_2 + v_3 \\
 &\vdots \\
 p_m &= p_{m-1} + \sum_{i=1}^k H_{s mi} S_i = p_{m-1} + v_m
 \end{aligned}$$

Algorithm 2.2: QC-LDPC encoding.

Step 1: Calculate As^T and Cs^T

Step 2: $ET^{-T} As^T$

Step 3: $p_1^T = ET^{-1} As^T + Cs^T$

Step 4: $p_2^T = As^T + Bp_1^T$

Step 5: $x = [s, p_1^T, p_2^T]$

Where s represents the message bits and p_1, p_2 are parity bits. Exponent T simply represents a transpose.

2.3 Decoding of LDPC Codes

In this literature review, we summarize the current state of research on LDPC decoding techniques and provide a comprehensive overview of the various LDPC decoding and LDPC coder techniques currently available. Various decoding techniques have been proposed for LDPC codes, including iterative decoding, belief propagation, and layered decoding. Iterative decoding is used to improve the accuracy of LDPC code decoding. The iterative decoding algorithm evaluates the reliability of each bit in the code by updating its value. The reliability of each bit is estimated by computing its probability of being 1 or 0 based on the probability of neighboring bits being 1 or 0 [23]. In contrast, belief propagation incorporates the use of probability distributions to update the sample values in an LDPC code [24].

Layered decoding is a variation of belief propagation making use of layered networks of neurons that compute probability values [25]. It is an effective technique for LDPC codes because it dramatically reduces computational complexity. This technique divides the operations performed during decoding into a series of independent levels or layers. Layered decoding provides an alternative to traditional iterative decoding that reduces the number of iterations and improves the BER. Another popular technique for LDPC decoding is the min-sum algorithm. This algorithm is based on the approximation of the max-log-likelihood function with the min-sum function. The min-sum algorithm is simpler than the belief propagation algorithm but suffers from higher error rates [26]. To improve the decoding performance of the min-sum algorithm, several modifications have been proposed, such as the use of iteratively reweighted least squares (IRLS) decoding [27]. More recently, neural network (NN) based approaches have been proposed for LDPC decoding. NN-based approaches, such as autoencoders, have shown promising results in improving decoding performance [28]. The use of NN-based approaches reduces the decoding complexity and improves the error-correction capability of LDPC codes. Hybridization of various LDPC decoding and LDPC coder techniques has been reported as the best approach to realizing high-performance, low-complexity codes [29]. In hybridization, the advantages of different decoding algorithms and encoder designs are combined to obtain a more robust LDPC code. Hybridization has been reported to improve the accuracy of the decoding algorithm and reduce the decoding complexity [30].

Different methods of decoding and coding for LDPC codes are based on belief propagation, iterative decoding, Gaussian elimination, and graph-based and layered decoders. Each approach has its advantages and disadvantages, and hybridization has been proven as the most effective approach for improving performance, reducing errors, and reducing computational complexity. Further research is required to improve the performance of LDPC codes in different applications. The decoding of LDPC codes is categorized into soft decision, hard decision, and hybrid methods [31]. Hybrid uses both decoding decisions interchangeably. In hard-decision decoding, the received data is assumed to be either 0 or 1, while in soft-decision decoding, the received data is represented as a probability distribution over the possible values. Soft decision and hard decision methods have the highest and lowest decoding complexity respectively. Although the soft decision has the highest complexity, it is powerful in error correction as compared to the hard decision [32].

Decoding LDPC codes involves a process called iterative decoding. The basic idea is to use the parity-check matrix of the code to iteratively correct errors in the received data. The parity-check matrix describes the relationships between data bits and the parity bits that are used to detect errors. LDPC decoding is an iterative process that involves passing the received data through a series of check nodes and variable nodes. The decoding process starts with an initial estimate of the data bits. This estimate is then passed through the check nodes to compute the syndromes, which represent the inconsistencies between the received data and the parity constraints. The variable nodes then update the probabilities of the individual data bits based on the syndromes. This process is repeated multiple times until either the error rate falls below a certain threshold, or a maximum number of iterations is reached. The threshold and maximum number of iterations are typically chosen based on the requirements of the specific application.

2.3.1 Soft Decision Decoding

Soft-decision decoding algorithms for LDPC codes are generally based on message-passing algorithms. The basic idea behind message-passing algorithms is to break down a complex problem into smaller sub-problems and solve them independently. In this way, the complexity of the problem is reduced, and a solution can be obtained more efficiently. The key concept in message-passing algorithms is the notion of messages, which are exchanged between different parts of the problem. Each message carries information about the state of the system

and is used to update the state of the system at the next iteration. The process of exchanging messages between different parts of the system is repeated iteratively until convergence is achieved [24]. Several types of message-passing algorithms exist, such as belief propagation, layered belief propagation, normalized min-sum and offset min-sum. We also call them Sum-Product Algorithms (SPA) because they operate on the Tanner graph representation of LDPC codes and iteratively exchange messages between variable nodes and check nodes, utilizing sum and product operations to propagate information and estimate the codeword. The messages in these algorithms represent the likelihood ratios (LLRs) of the possible values of the variables given the received data and the parity constraints. The messages are updated iteratively until a convergence criterion is met, typically when the likelihood of the transmitted message is maximized.

The SPA algorithms are both computationally efficient and can handle high code rates and large block lengths. They are also very robust to noise and can achieve performance close to the Shannon limit. One variant of the SPA algorithm that has been particularly successful for LDPC decoding is the min-sum algorithm, which approximates the message-passing updates using the min and sum operations instead of multiplication and addition. The min-sum algorithm can be implemented using simple hardware and is well-suited for low-power applications. Generally, the SPA looks at the probabilities of each bit as an input, and that is what makes the algorithm be soft decision procedure. The probabilities of each bit are calculated, which enables the decoder to decide which bit to start with [32]. The SPA probabilities are presented in the form of LLRs given by equation 2.4.

$$LLR(x) = \log \left\{ \frac{P(x = 0)}{P(x = 1)} \right\} \quad (2.4)$$

The algorithm is described as follows; Extrinsic messages are exchanged between check nodes j and bit nodes i , represented by $E_{j,i}$. The $E_{j,i}$ provides the probability of bit ci which is assumed to be 1. The value of ci must satisfy the parity check equation of j . The probability of the old number 1 is represented in equation 2.5.

$$P_{j,i}^{ext} = \frac{1}{2} - \frac{1}{2} \prod_{i' \in B_j, i' \neq i} (1 - 2P_{i'}^{int}) \quad (2.5)$$

The product of the sum-product decoder reduces significantly when we apply equation 2.5 above to find the product of the probabilities. The extrinsic results from check nodes j to variable nodes i are represented in equation 2.6 below.

$$E_{j,i} = LLR(P_{j,i}^{ext}) = \log \left[\frac{1 - P_{j,i}^{ext}}{P_{j,i}^{ext}} \right] \quad (2.6)$$

The equation has been worked out in [32], and the final equation for the decoder of LLR as the summation of the individual LLRs is equation 2.7.

$$L_i^{total} = L_i + \sum_{j \in A_i} E_{ji} \quad (2.7)$$

It is difficult to tell if the received bits are given by the signs of the L_i^{total} . Equation (2.8) is used to investigate whether the parity check equations are fulfilling the requirements of the system. For instance, if the equation does not satisfy, then update $M_{j,i}$.

$$L_i^{total} = \sum_{j^i \in A_{i,j} \neq j} E_{j^i i} + L_i \quad (2.8)$$

This procedure estimates a-posteriori bit probabilities of the received bits as LLRs. The decoder stops if $C \cdot H^T = \mathbf{0}$ or permits most of an extreme number of emphases accomplished. The decoder is introduced by setting up all Variable Nodes (VN) messages to $M_{j,i}$ to equation 2.9.

$$L_i = L(c_i | y_i) = \log \left(\frac{P_r(c_i = 0 | y_i)}{P_r(c_i = 1 | y_i)} \right) \quad (2.9)$$

2.3.1.1 Belief Propagation Decoding Algorithm

The algorithm works by iteratively passing messages between the nodes of the code, updating their beliefs about the value of each bit. The algorithm has proven to be effective in achieving near-optimal performance in decoding LDPC codes. The algorithm operates on a bipartite graph, where one set of nodes represents the input data bits, and the other set represents the parity check equations. Each node is connected to the nodes on the other side of the graph,

forming a bipartite structure. The algorithm starts with an initial estimate of the state of each input data bit. These estimates are then used to calculate the probability of each parity check equation being satisfied. This information is used to update the estimates of the input data bits, and the process is iterated until satisfactory decoding is achieved [24].

During each iteration of the algorithm, messages are passed between the nodes of the graph. There are two types of messages: check-to-bit messages and bit-to-check messages. The check-to-bit messages carry information from the parity check equations to the input data bits, and the bit-to-check messages carry information from the input data bits to the parity check equations [6],[33].

2.3.1.2 Layered Belief Propagation Algorithm

LDPC Layered belief propagation (LBP) algorithm is a message-passing algorithm for decoding LDPC codes. It is a multi-layered algorithm that aims to estimate the likelihood of each bit in a received word. The algorithm iteratively updates messages between the variable nodes and check nodes in the graph representation of the LDPC code until a convergence criterion is met. The LBP algorithm utilizes a belief propagation algorithm to update the messages between the variable nodes and the check nodes. The algorithm operates on a bipartite graph where the variables are represented as nodes on one partition and the checks are represented as nodes on the other partition. Each edge in the graph represents a parity constraint that links a variable node to the check node. The regularization parameter, usually a scalar, determines the strength of the correction, this is important as it indicates the amount of protection that is needed [34].

The LBP algorithm uses a layered approach to updating the messages. The messages are updated in an outer loop, with each inner loop representing a layer or level of the LDPC code, from the outermost to the innermost layer. The outer layer represents the input bits or channel observations, while the innermost layer represents the parity checks. The algorithm begins by initializing the message values according to the input bits. Then, in each iteration, the messages are passed from the variable nodes to the check nodes and back to the variable nodes again. The messages are updated using the sum-product rule and passed iteratively through the layers until they converge, that is when the difference between the messages of adjacent iterations is smaller than a predefined threshold. The LBP algorithm is an efficient algorithm that provides good decoding performance, especially in the low signal-to-noise

ratio region. It is also scalable to large code sizes and can be used with different decoding techniques [35].

2.3.1.3 Normalized Min Sum Algorithm

The normalized min-sum algorithm is an iterative message-passing decoding algorithm for LDPC codes. This algorithm works with the assumption that the entries of each parity-check equation form a sparse matrix. The algorithm starts with initial messages between variable nodes and check nodes, which are represented by the variable-to-check and check-to-variable matrices, respectively. The messages are computed iteratively until a stopping criterion is met. In each iteration, the algorithm performs the following steps [36]:

Update variable-to-check messages: For each variable node i , the algorithm updates its message to each check node j by computing a weighted sum of the messages from other check nodes to which i is connected. The weights are obtained by subtracting the minimum absolute value from all the other values and scaling the resulting values by a factor γ . The value of γ depends on the number of check nodes connected to i and the code rate. Update check-to-variable messages: For each check node j , the algorithm updates its message to each variable node i by computing the sum of the messages from all other variable nodes connected to j , except i . If a message from a variable node i to a check node j is updated in step 1, the updated value is used in the computation of the check-to-variable message.

Perform a hard decision: After a sufficient number of iterations, the algorithm performs a hard decision based on the computed messages to declare the transmitted bits. The normalized min-sum algorithm has been shown to achieve near-optimal performance for LDPC codes with moderate to high error rates [37]. However, it may suffer from error floor phenomena at very low error rates. Several enhancements to the algorithm have been proposed to mitigate this issue, including the offset min-sum algorithm and flipping algorithm [38] - [39].

2.3.1.4 Offset Min Sum Algorithm

The Offset Min-Sum algorithm is one of the popular decoding algorithms. In 5G mobile communications, an improved version of the Offset Min-Sum algorithm for LDPC codes is presented [40], demonstrating superior performance in simulations despite a slight increase in complexity compared to the original Min-Sum algorithm. Nonetheless, the Offset Min-

Sum algorithm remains a powerful decoding algorithm. The Min-Sum decoding algorithm is a variant of the Sum-Product Algorithm that achieves a good balance between complexity and performance in LDPC codes [41]. The Min-Sum algorithm works on the basis of the belief propagation method, where the messages are exchanged between the variable nodes and the check nodes [42]. The algorithm searches for a valid codeword by iteratively updating the messages until convergence is reached. One of the challenges in implementing Min-Sum decoding is managing the computation of the message entries, especially for high-density matrices with many non-zero entries, which can lead to high computational complexity [43]. The Offset Min-Sum algorithm is a modification of the Min-Sum algorithm that reduces the complexity of the computation while maintaining similar decoding performance [44]. The Offset Min-Sum algorithm introduces an offset parameter to shift the initial message values to eliminate the need for the normalization operation in the standard Min-Sum algorithm. Moreover, the Offset Min-Sum algorithm allows for efficient implementation on parallel platforms [45].

The Offset Min-Sum algorithm works by initially setting the messages from the variable nodes to be the logarithm of the LLRs of the received symbols [46]. The messages from the check nodes are then computed by summing over the incoming message values and subtracting the minimum value. The resulting message is then shifted by an offset value that depends on the largest incoming absolute value and the gain parameter γ . The offset value allows for faster computation by eliminating the need for normalization, reducing the computational complexity of the algorithm. The Offset Min-Sum algorithm has been demonstrated to provide similar or better decoding performance compared to the standard Min-Sum algorithm while requiring fewer computational resources. Furthermore, the Offset Min-Sum algorithm can be efficiently implemented on parallel and distributed platforms, making it an attractive option for implementing LDPC code decoding in high-performance computing systems [46]-[49]. The LDPC Offset Min-Sum algorithm is a modification of the Min-Sum decoding algorithm that reduces the computational complexity while maintaining similar decoding performance. The algorithm introduces an offset parameter that eliminates the need for normalization, allowing for efficient implementation on parallel platforms. The Offset Min-Sum algorithm has been shown to provide good decoding performance and is an excellent option for implementing LDPC code decoding in high-performance computing systems.

2.3.2 Hard Decision Decoding

One of the best examples of hard decision decoding is the bit-flipping algorithm [32]. It applies the bit-flipping algorithm to pass messages in a tanner graph between the edges. The message node conveys information to the check node that the bits available at the message node are either zero or one. The check node sends back the response. The response is triggered by using the parity check equation, which is based on the constrained sum of bits available to the check node [50]. Let the codeword be $C = [11001000]^T$ and the received codeword be $Y = [10001000]^T$ which implies that bit C_2 is flipped.

$$\begin{bmatrix}
 0 & 1 & 0 & 1 & 1 & 0 & 0 & 1 \\
 1 & 1 & 1 & 0 & 0 & 1 & 0 & 0 \\
 0 & 0 & 1 & 0 & 0 & 1 & 1 & 1 \\
 1 & 0 & 0 & 1 & 1 & 0 & 1 & 0
 \end{bmatrix}$$

Figure 2 - 1: The parity check matrix H

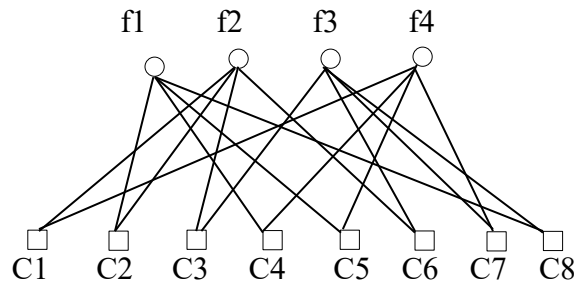


Figure 2 - 2: Parity check matrix and the corresponding Tanner graph

Figure 2-1 illustrates the parity check matrix and the corresponding tanner graph in Fig.2-2 used on a decoding algorithm. The steps used in the bit-flipping algorithm are given below.

Table 2 - 1: Overview of messages received and sent by the check nodes.

Check nodes	Activities				
	f_1	Receive	$C_2 \rightarrow 0$	$C_4 \rightarrow 0$	$C_5 \rightarrow 1$
	Send	$1 \rightarrow C_4$	$1 \rightarrow C_4$	$0 \rightarrow C_5$	$1 \rightarrow C_8$
f_2	Receive	$C_1 \rightarrow 1$	$C_2 \rightarrow 0$	$C_3 \rightarrow 0$	$C_6 \rightarrow 0$
	Send	$1 \rightarrow C_1$	$0 \rightarrow C_2$	$0 \rightarrow C_3$	$0 \rightarrow C_6$
f_3	Receive	$C_3 \rightarrow 0$	$C_6 \rightarrow 0$	$C_7 \rightarrow 0$	$C_8 \rightarrow 0$
	Send	$0 \rightarrow C_3$	$0 \rightarrow C_6$	$0 \rightarrow C_7$	$0 \rightarrow C_8$
f_4	Receive	$C_1 \rightarrow 1$	$C_4 \rightarrow 0$	$C_5 \rightarrow 1$	$C_7 \rightarrow 0$
	Send	$1 \rightarrow C_1$	$0 \rightarrow C_4$	$1 \rightarrow C_5$	$0 \rightarrow C_7$

Table 2 - 2: Message node decisions for hard decision decoder.

Message Nodes	Y_i	Message from check node		Decision
C_1	1	$f_2 \rightarrow 0$	$f_4 \rightarrow 1$	1
C_2	0	$f_2 \rightarrow 1$	$f_4 \rightarrow 1$	1
C_3	0	$f_2 \rightarrow 1$	$f_4 \rightarrow 0$	0
C_4	0	$f_1 \rightarrow 1$	$f_4 \rightarrow 0$	0
C_5	1	$f_1 \rightarrow 0$	$f_4 \rightarrow 1$	1
C_6	0	$f_2 \rightarrow 1$	$f_4 \rightarrow 0$	0
C_7	0	$f_3 \rightarrow 0$	$f_4 \rightarrow 0$	0
C_8	0	$f_1 \rightarrow 1$	$f_4 \rightarrow 0$	0

Algorithm 2.8: Hard decision bit flipping.

Step 1: All message nodes send a bit message to their connected check nodes. In this example, C_1 sends a 1 to f_2 and f_4 as shown in Table 2-1.

Step 2: Every check node calculates the response to send to their connected nodes using the message they received from Step 1. These calculations are achieved by means of a parity check equation. If the calculated sum is equal to zero, then check nodes send the same bit received from the message node but if the sum is not zero then the check node flips the bit and resends it back to the message node.

Step 3: The message nodes then use the message they get from the check nodes to decide if the bit is a zero or a one, deciding by majority rule. The message node then sends the bit decided to their connected check nodes as illustrated in Table 2-2.

Step 4. Repeat step 2 and exit if complete or continue until the maximum number of iterations is reached.

2.4 Adaptive Modulation

Adaptive modulation is a signal processing technique that improves the spectral efficiency of wireless communication systems by allowing the transmitted signal to vary the modulation type and symbol rate to fit the changing conditions of the communication channel [51]. This section aims to provide an overview of the most important contributions to adaptive modulation research and their impact on technology.

2.4.1 Early Developments

The earliest research into adaptive modulation dates back to the 1960s. In 1963, Hewitt et al. [52] proposed a modulation scheme that dynamically adjusted the carrier frequencies and phases of a communication signal to minimize the effects of multipath fading. Although their approach was quite crude by modern standards, they were the first to demonstrate the potential of adaptive modulation for wireless communication.

2.4.2 Advancements in Adaptive Modulation

Researchers in the 1970s began exploring more sophisticated forms of adaptive modulation. In 1974, Ghorayeb et al. [53] proposed a coding scheme that combined adaptive modulation with convolutional coding. Their method used a feedback loop to adjust the modulation rate and error correction level based on the measured SNR of the channel, greatly improving the error performance of wireless systems. In the 1980s, efforts focused on improving real-time performance. Simon et al. [54] introduced a computationally efficient adaptive modulation algorithm in 1987. Their method employed a look-up table of pre-calculated modulation levels and corresponding BERs, allowing for rapid adjustments to changing conditions. This approach was widely adopted in commercial wireless systems.

2.4.3 Adaptive Modulation in MIMO Systems

In the 1990s, researchers explored the use of adaptive modulation in multiple-input multiple-output (MIMO) systems. Goldsmith et al. [55] proposed a space-time coding scheme in 1998 that combined adaptive modulation with spatial diversity to improve capacity and reliability. Subsequent work in the 2000s focused on refining adaptive modulation in MIMO systems to maximize throughput subject to power constraints [56].

2.4.4 Recent Advances and Energy Efficiency

Recent research has focused on improving the energy efficiency of adaptive modulation systems. Ma et al. [57] proposed an energy-efficient adaptive modulation scheme in 2013 that minimized total energy consumption while meeting Quality of Service (QoS) constraints. Additionally, novel algorithms such as adaptive modulation, power control, and clipping (MPC) have been developed to address drawbacks like high Peak to Average Power Ratio (PAPR) in OFDM systems [58]. These techniques have shown promise in improving system performance while addressing practical concerns. The authors in [58] have proposed an adaptive modulation algorithm and investigated the application of the proposed adaptive modulation algorithm when used together with LDPC codes. They have used the bit and power load algorithm to minimize the BER of OFDM sub-carriers which are in deep fading because those sub-carriers determine the BER of the system. Therefore, they have expressed the BER as a function of power p_i and b_i as follows

$$p(e_i) = f(r_i, b_i) = f(g_i, p_i, b_i), i = 1, 2, \dots, K \quad (2.10)$$

Whereby $f(\cdot)$ function is determined by the modulation scheme. $SNR_i = r_i = g_i, p_i$ is the SNR of subcarrier i , and $g_i = |h|^2/\sigma^2$ is the gain ratio to noise power which gives the channel state of the i the subcarrier. Besides the power and bit loading which is too complicated, they have integrated the Belief propagation LDPC decoder to adapt to each and every subchannel state by calculating the LLR using equation.

$$LLR(b_i) = \log \frac{\sum_{s \in \beta(b_i=0)} \exp(-(|z - h_i s|^2)/2\sigma^2)}{\sum_{s \in \beta(b_i=1)} \exp(-(|z - h_i s|^2)/2\sigma^2)} \quad (2.11)$$

Whereby z is the received signal, s is a point of the transmitted constellation of QAM, h_i is the channel gain, σ is the Gaussian noise variance, and β ($b_i = 0$) represents the subconstellation of β with the bit b_i equal to zero. This equation calculates for each and every subchannel thereafter, the LDPC decoder will decode the LLR values. Adaptive Modulation combined with OFDM could improve the system by using high-order modulation schemes such as 256-QAM, and 128-QAM at low SNR [59]. Presented in [59] is a novel algorithm with a new adaptive modulation form to improve the performance of OFDM for 4G systems. The algorithm is called adaptive modulation, Power Control, and Clipping (MPC). This technique addresses the main disadvantage of OFDM which is high Peak to Average Power Ratio [PAPR], linearity concerns, and phase noise. The variation of the envelope of the multi-carrier signal can be defined by PAPR which is given below as

$$PAPR = \frac{Max}{E\{|x(t)|^2\}} \quad (2.12)$$

Another widely used form of adaptive modulation is whereby there is a look-up table and the channel state information feedback, SNR-based adaptive modulation. The parameter and feedback mechanism implemented in [60] is as follows. The transmitter controls the process of changing the modulation but the whole process depends on the receiver which continually assesses the SNR. The receiver assesses the SNR and calculates the BER rate, it then compares the current BER to the target BER and picks up the mode or modulation scheme that yields the greatest throughput while staying inside the BER target limits. Once the best mode has been picked according to Table 2.3, it feeds back that information to the transmitter to inform the transmitter that a modification can be performed and thereafter reconfigure itself to the selected mode and be ready for the next frame.

Table 2 - 3: Parameter Adaptation Thresholds

Mode	Modulation	Thresholds
1	BPSK	SNR < 12 dB
2	QPSK	12 dB < SNR < 16dB
3	16 QAM	12 dB < SNR < 16 dB
4	64 QAM	SNR > 16 dB

Threshold decision adaptive modulation and coding schemes for OFDM Communications abbreviated as TD-AMC Technique for OFDM systems is proposed in [61]. This technique changes the order of modulation in the transmitter on each OFDM subcarrier separately depending on the BER on that subcarrier. The subcarrier measurements are done by the receiver as in most systems using the feedback adaptive modulation technique. The order of modulation is decided according to the change in BER (Δ BER) level on the subcarrier. Table Thresholds are shown below in Table 2.4.

Table 2 - 4: Modulation order and BER thresholds

Measure of BER	Thresholds	Modulation Order
40%	< Δ BER	4-PSK
40%	$\geq \Delta$ BER > 30%	8-PSK
30%	$\geq \Delta$ BER > 20%	16-PSK
20%	$\geq \Delta$ BER > 10%	32-PSK
10%	$\geq \Delta$ BER	64-PSK

The adaptation process window takes 100 frames, basically, they measure the BER on 100 frames if the change needs to happen based on the current 100 frames measured then, it will be compared to the previous 100, and decides if a change needs to be implemented. The authors have proposed an indicator to evaluate the overall performance. The indicator proposed is p_indic , It includes the BER, the spectral efficiency, and the overhead. It evaluates these parameters using equation 2.20.

$$p_i ndic = \sum_i \beta_i (\alpha_1 PBERE + \alpha_2 PSEE - \alpha_3 POE) \quad (2.20)$$

PBERE: Percentage BER Enhancement over the M-ary.

PSEE: Percentage Spectral Efficiency Enhancement over the M-ary.

POE: Percentage Overhead, due to changing the order of modulation, over the M-ary.

α 's : weighting factor.

β_i : weighting factor is chosen from Gaussian distribution for the SNR

i : take all possible values of M.

It is proposed to take $\alpha_1 = \alpha_2 = \alpha_3 = 1$, to include the bandwidth overhead, due to sending the CSI, in the *PSEE*.

2.4.5 Adaptive Modulation and Coding for NTN Network

While AMC thresholds are commonly associated with terrestrial wireless communication systems, their principles and application can also be extended to satellite communication networks. In the context of our research, which focuses on Non-Terrestrial Networks (NTN) and their integration with 6G mobile communication networks, the utilization of AMC thresholds is relevant and justified. As NTN networks incorporate satellite communication links alongside terrestrial links, the optimization of modulation and coding schemes becomes crucial for maximizing throughput and ensuring reliable communication.

Furthermore, the deployment of NTN networks introduces unique challenges and considerations, such as the propagation characteristics of satellite links and the need to account for atmospheric effects. By incorporating AMC thresholds tailored to the specific characteristics of satellite communication channels, we can effectively optimize system performance and adapt to varying channel conditions. Therefore, while the AMC thresholds discussed in our research may not be explicitly labeled for satellite communication, their application to NTN networks, which include satellite links, is both relevant and beneficial

for achieving the objectives of our study.

2.5 Orthogonal Frequency Division Multiplexing

OFDM is used in state-of-the-art communication devices because it is effective in solving the intersymbol interference (ISI) caused by a dispersive channel [62]. Another major advantage of OFDM is that it transfers the complexity of transceivers from analog to digital. The basic functions of OFDM are Fast Fourier Transform (FFT) and its inverse, the IFFT.

2.5.1 FFT and IFFT

The IFFT is the main block at the transmitter, and the FFT is the main block at the receiver. The input to the IFFT is a complex modulated signal, and the output of the FFT is also a complex signal. The Cyclic Prefix (CP) is appended after IFFT and removed before the FFT. The input signal to the IFFT is a complex modulated vector $X = [X_0 + X_1 + X_2 + \dots + X_{N-1}]^T$. X represents data to be carried in a subcarrier, with a length N where N is the size of the FFT. For instance, X_n represents data to be carried in the n th subcarrier. The output of the FFT is a time-domain complex vector $x = [x_0 + x_1 + x_2 + \dots + x_{N-1}]^T$.

The IFFT is given by equation 2.13.

$$x_m = \frac{1}{\sqrt{N}} \sum_{n=0}^{N-1} X_n \exp\left(\frac{j2\pi nm}{N}\right)$$

for $0 \leq m \leq N$ (2.13)

The FFT is given by equation 2.14

$$x_n = \frac{1}{\sqrt{N}} \sum_{m=0}^{N-1} X_m \exp\left(\frac{-j2\pi nm}{N}\right)$$

for $0 \leq m \leq N$ (2.14)

The IFFT/FFT transform pair has the important advantage that the discrete signals at the input and output of the transform for each and every symbol have the same total energy and average power. OFDM systems use the CP as the guard interval to combat Inter Symbol Interference (ISI) and Inter Carrier Interference (ICI), however, the CP reduces the transmission efficiency

of the system mostly channels with Channel Impulse Response (CIR) such as hilly terrain channels [63]. On the other hand, it is known that time-varying channels give rise to ICI. The research in [63] has shown that in order to achieve the SNR of 20 dB for a slow fading channel, a half-length of CIR is enough for the CP. This briefly explains the role of the CP which is used by all OFDM systems but the length of the CP has to be selected carefully. Let's consider the OFDM system, the receiver first removes the CP and then does the FFT process to get Y in the frequency domain at time i^{th} . If the length of CP, say we defined it as P is shorter than the length of CIR then we get the interference so, the output signal will be given by equation 2.15.

$$\begin{aligned}
 Y_1 &= WH_{ICI}W^HX_i + WH_{ISI_{CP}}W^HX_{i-1} + Z \\
 &= Y_s + Y_{ICI} + Y_{ISI_{CP}} + Z
 \end{aligned} \tag{2.15}$$

2.6 The f-OFDM system

The f-OFDM was first introduced by Farhang and Khaledi in 2010 as a method to reduce the filter complexity of OFDM systems while maintaining good spectral containment. In their work, they proposed a low-complexity f-OFDM scheme that uses Filtered Impulse Response (FIR) filters to smooth the frequency response of the OFDM system [64]. The performance of the proposed f-OFDM scheme was evaluated and compared to that of the traditional OFDM scheme using simulations. They found that f-OFDM provided superior performance in terms of reducing the peak-to-average power ratio (PAPR) and ISI. Since then, f-OFDM has gained significant attention from the research community due to its potential to improve the performance of OFDM-based systems.

Researchers have proposed various methods to optimize the design and performance of f-OFDM systems. One of the main challenges of f-OFDM is the choice of the FIR filter coefficients that determine the frequency response of the system. Several researchers have proposed different design methods for the FIR filters used in f-OFDM systems. In 2011, Researchers [65] proposed a design method for FIR filters based on the minimization of the mean square error (MSE) between the frequency response of the filter and a desired target frequency response. They formulated the design problem as a convex optimization problem

that could be solved using an iterative algorithm. The proposed filter design algorithm was shown to significantly reduce ISI and PAPR in f-OFDM systems [65].

In 2016, Researchers [66] proposed a new method for designing FIR filters based on the maximization of the SNR of the f-OFDM system. They formulated the filter design problem as a nonlinear optimization problem that was solved using a particle swarm optimization (PSO) algorithm. The proposed filters were shown to outperform other commonly used filters in terms of SNR and BER performance [66]. Another area of research in f-OFDM is the design of receiver algorithms that can effectively decode the transmitted signal. Since f-OFDM uses FIR filters that introduce a delay in the system, traditional OFDM receiver algorithms such as the cyclic prefix (CP) insertion technique are not applicable. Researchers have proposed various receiver algorithms that can effectively decode the f-OFDM signal.

In 2015, Researchers [56] proposed a receiver algorithm for f-OFDM based on the weighted least squares (WLS) technique. The proposed algorithm was shown to effectively decode the f-OFDM signal and outperform traditional OFDM receivers in terms of BER performance [56]. In 2019, Researchers [57] proposed a novel receiver algorithm for f-OFDM based on the linear minimum mean square error (LMMSE) technique. The proposed algorithm was shown to mitigate the ISI introduced by the FIR filters and significantly improve the BER performance of f-OFDM systems [57].

f-OFDM is a promising technology that can significantly improve the performance of OFDM-based systems. Researchers have proposed various methods to optimize the design and performance of f-OFDM systems, including filter design algorithms and receiver algorithms. The development of f-OFDM technology will continue attracting researchers' attention in the field of wireless communication in the years to come.

2.7 Ka-band Satellite Channel Model

Researchers have been working tirelessly to improve the performance of Ka-band through various means including but not limited to, signal processing techniques, modulation schemes, and the deployment of new communication systems. The aim of this literature review is to provide a comprehensive understanding of the research that has been done to improve the performance of Ka-band. One of the earliest works to improve the performance of the Ka-band was conducted by Juha Kyulinkka and Kari Halonen in 1997 [67]. They

conducted a study on the effects of rain attenuation on Ka-band satellite communication systems. The research showed that Asynchronous Transfer Mode (ATM) based modulation techniques could mitigate the effect of rain attenuation on the performance of Ka-band communication systems. In 2003, researchers Yagos M. Jahshan and A. R. Al-Ali conducted a study of Ku-band and Ka-band satellite communication systems [68]. The research focused on the evaluation of the outage probability and the BER for both frequency bands under different weather conditions. The results showed that Ka-band was more affected by rain than the Ku band, and therefore, the researchers proposed the use of a combination of FEC coding and interleaving to improve the performance of the Ka-band.

Signal processing techniques have also been successfully applied to improve the performance of the Ka-band. In a study conducted by Yonghong Zhang, Shan Zhang, and Shaoqian Li in 2011 [69], they proposed a novel technique known as the eigenvalue decomposition-based blind source separation for mitigating the effects of multipath propagation in the Ka-band communication systems. The proposed technique showed significant improvement in the performance of Ka-band communication systems in the presence of multipath propagation. In 2013, researchers Yue Li and Zhaowei Qu proposed a technique called adaptive joint coding and modulation for Ka-band satellite communication systems [70]. This technique was aimed at improving the performance of the Ka-band by adapting the modulation and coding scheme based on the weather conditions. The research showed that the proposed technique achieved a higher throughput and lower BER compared to conventional modulation and coding schemes.

The literature review shows that researchers have made significant progress in improving the performance of Ka-band communication systems. The studies reviewed in this research study have shown that signal processing techniques, modulation schemes, and weather adaptive techniques are effective in mitigating the effect of atmospheric conditions on the performance of the Ka-band. It is expected that with continued research, Ka-band will continue to evolve and achieve better performance in the future. Ka-band radio frequency is used mainly in satellite communication systems. The main advantage of the Ka-band over other frequency bands is its ability to transmit large amounts of data over a short period of time due to its high bandwidth. However, the performance of the Ka-band is limited by atmospheric effects such as water vapor, atmospheric turbulence, and rain attenuation [71].

One of the ways to model the Ka-band is to find the probability of the signal envelope and signal phase which can be described in terms of statistical models [72]. In this research, we used the measurements from the research paper [72] in which they collected data from the Olympus satellite in Ottawa, Canada. The channel characteristics of fixed satellite communication are affected by weather conditions, whereas the mobile satellite channel is affected by weather and shadowing. These models describe both fixed and mobile satellite channels at Ka-band. Fixed satellite channel characteristics signal envelope and signal phase are modeled as Gaussian distribution and the shadowing and multipath can be modeled as Rician and Rayleigh fading.

The two fading processes are independent whereby the combined probability density function (pdf) of the signal envelope and the signal phase is given by

$$p(r) = p_w(r).p_s(r) \quad (2.16)$$

$p_w(r)$ is the signal envelope pdf due to weather conditions, it is modeled as Gaussian distribution.

$p_s(r)$ is the signal envelope pdf due to fading and shadowing.

Similarly, the combined signal phase model is given by

$$p(\emptyset) = p(\emptyset_w + \emptyset_s) \quad (2.17)$$

\emptyset_w is the signal phase caused by weather conditions.

\emptyset_s is the signal phase caused by fading and shadowing

$p(\emptyset)$ is Gaussian distribution.

Ka-band Land Mobile Satellite (LMS) channel with a focus on rain attenuation and other weather impairments in the equatorial zone is studied in [73]. They investigate the statistical characteristics of the rain attenuation in the equatorial zone and compare it with Loo's Ka-band weather LMS model. This enables them to propose a more reasonable LMS channel model that incorporates weather impairments. The proposed LMS model is based on Lutz's LMS channel model. Loo's model considered the weather impairments but weather effects

on received signal amplitude are not correctly studied which motivated the study in [73] to propose a new Ka-band weather LMS channel model. They investigate weather effects on PDF of received signal amplitude under various weather conditions: rain, intermittent rain, light rain, and thunderstorms. Rain attenuation measurements were taken in Singapore which is located in the equatorial zone and thus experiences a tropical climate of heavy rains. Singapore's rain rate falls between the ITU-R rain climate zone N & P. Ka-band rain attenuation is calculated using the methods proposed in ITU-R PN.837-1. $A_p = \gamma_R \cdot L_e$, γ_R depends on the frequency and intensity R_p (mm/h) of the rain. p is the value of exceeding attenuation p percentage of the time. The long-term statistics of rain attenuation are modeled as a lognormal process.

$$P_L(L) = \frac{1}{\sqrt{2\pi}\sigma_d L} \exp\left[-\frac{(\ln L - m_d)^2}{2\sigma_d^2}\right] \quad L \geq 0 \quad (2.18)$$

L , m_d , and σ_d are in dB.

2.8 Integration of LDPC codes, OFDM, f-OFDM, and Adaptive Modulation

Combining LDPC codes, adaptive modulation, OFDM, and f-OFDM constitutes a comprehensive strategic approach to address the limitations identified in the current research, as presented in [3]. This approach effectively tackles the challenges posed by Ka-band interference. LDPC codes provide robust error correction, adaptive modulation dynamically adjusts modulation schemes and coding rates, while OFDM and f-OFDM enhance spectral efficiency and resilience against interference. This integrated approach optimizes system performance by leveraging the complementary strengths of each technique. LDPC codes mitigate interference-induced errors, adaptive modulation maximizes throughput by adapting to changing channel conditions, and OFDM/f-OFDM ensures efficient spectrum utilization and combat interference effects. Together, these techniques synergize to create a robust communication system capable of maintaining reliable connectivity in the face of challenging Ka-band environments, ensuring high-performance transmission even under adverse conditions.

2.9 Summary

The literature has addressed the research question: "How can we mitigate the effect of rain fade in the Ka-band?" After conducting a thorough review of papers in this field of study, we identified a gap in the application of adaptive modulation, which led us to investigate means of improving the performance of LDPC codes in reducing rain fade in the Ka-band. Adaptive modulation, an important signal processing technique, allows wireless systems to adapt to changing communication conditions. Numerous studies in the literature have explored this technique and its benefits.

Motivated by the aforementioned literature, we decided to employ f-OFDM to further enhance the system. Recent advances in studies have demonstrated that f-OFDM is a promising technology and the way forward. It has the potential to significantly improve the performance of OFDM-based systems, making it an ideal choice for our research. Moreover, the literature highlights that applying LDPC codes can enhance communication in the Ka-band frequency. In our study, we apply LDPC codes and refer to the literature to identify the best method of decoding. Soft decoding algorithms are recommended by the literature as the most effective approach for LDPC decoding.

CHAPTER THREE

Modeling and Design of the System

3.1 Introduction

The saturation of lower frequency bands and the growing demand for high data rate services have presented the need to design future systems at Ka-band frequency [3]. Ka-band frequencies range from 20 to 30 GHz which makes the signal more susceptible to weather impairments and shadowing as compared to lower band frequencies. Rain attenuation is a major problem in satellite communications operating at Ka-band, it causes major signal degradation because the raindrop is about the size of the Ka-band frequency wavelength. Rain fade causes scattering attenuation in the direction of propagation. It is a frequency-nonspecific, slow time-varying channel [4]. Researchers in [3] and [4] have used LDPC codes to overcome the rain attenuation in the Ka-band satellite communication, but their system used BPSK and fixed QAM modulation schemes which resulted in limited spectral efficiency and data rates, and susceptibility to interference. These limitations lead to poor system performance meaning that even if you are using LDPC codes, you still do not explore the full capability of the system. To overcome these problems, we propose adding adaptive modulation and f-OFDM into the system. LDPC codes have become very popular due to their ability to perform very close to the Shannon limit (channel capacity). We have integrated adaptive modulation because it provides both mobile and fixed users with the best compromise among several factors, such as robustness against transmission errors, spectral efficiency, and power consumption [74]. The modern system must include state-of-the-art multiplexing technology. For this reason, we propose using f-OFDM, which is an essential building block in 5G. f-OFDM addresses the problem of basic OFDM signal clipping [75]. Therefore, we are applying f-OFDM to further improve the system performance.

3.2 The System Model

3.2.1 LDPC Codes

LDPC codes were developed by Gallager in the 1960s for his doctoral thesis. They were ignored until Turbo codes were introduced in 1993, since then, LDPC codes have become very popular and are now one of the intensely studied areas in FEC coding [76]. LDPC codes exhibit excellent performance with iterative decoding, approaching the Shannon limit. LDPC codes are used in valuable applications where reliable and low BER is required such as Digital

Video Broadcast Satellite-Second Generation (DVB-S2), fourth generation for mobile communications (4G), and worldwide Interoperability for Microwave Access (WiMAX) [77]. LDPC codes are made up of a parity check matrix H of m by n whereby m is the number of rows and n is the number of columns. The code rate is $R = (n-m)/n$. Each row and column of a regular LDPC code parity check matrix H contains ρ nonzero elements λ nonzero elements respectively [3]. LDPC codes are divided into two categories namely regular and irregular. Regular LDPC codes have a uniform row and column weight and irregular LDPC codes have a different number of nonzero elements in a row and column. The row and column weight refers to the number of ρ nonzero elements in a row and the number of λ nonzero elements in a column. The parity check matrix H is said to be sparse if it has a small number of ρ nonzero elements and λ nonzero elements, if the number is small compared to a large H Matrix, the code performance will be good. Irregular LDPC codes are described by degree distribution or edge degree [78]. The matrix H has dimensions m by n having column weight i degree distribution. The column degree distribution is given by equation 3.1 and the row degree distribution is given by equation 3.2 as described in [78].

$$v_i = \frac{\text{number of columns with weight } i}{n} \quad (3.1)$$

$$h_i = \frac{\text{number of rows with weight } i}{m} \quad (3.2)$$

Both equations must fulfil the constraints below.

$$\sum_i v_i = 1 \quad \sum_i h_i = 1$$

We say the node has d degree if it has d branches connected to it. Regular LDPC codes have the same variable nodes degree d_v and check nodes degree d_c . Irregular LDPC codes variable and check nodes are characterized by degrees varying according to a distribution. The degree distributions are polynomials denoted by equations 3.3 and 3.4 as described in [77].

$$\lambda(x) = \sum_{i=2}^{d_v} \lambda_i x^{i-1} \quad (3.3)$$

$$\rho(x) = \sum_{i=2}^{d_c} \rho_i x^{i-1} \quad (3.4)$$

λ_i and ρ_i correspond to the fraction of branches in the graph connected to degree d_v variable nodes and degree d_c check nodes [77]. Supposed a transmitted codeword is s and the received codeword is x . The parity check equation is given by equation 3.5 as described in [80].

$$H \cdot x^T = 0 \quad (3.5)$$

Where x^T is the transpose of the codeword and H is the parity check matrix [79],[80]. The purpose of parity check matrix H is to verify if a given codeword satisfies all parity check equations.

$$H = \begin{bmatrix} 1 & 0 & 1 & 0 & 0 & 1 \\ 1 & 0 & 1 & 0 & 1 & 0 \\ 0 & 1 & 0 & 1 & 0 & 1 \end{bmatrix} \rightarrow \begin{cases} C1 + C3 + C6 = 0 \\ C1 + C3 + C5 = 0 \\ C2 + C4 + C6 = 0 \end{cases} \quad (3.6)$$

C represents check nodes; thus, we can represent check nodes of equation 3.6 as $\vec{C} = (C1, C2, C3, C4, C5, C6)$. LDPC codes can be represented graphically using a Tanner graph in Figure 1 for a parity check matrix H of equation 3.6. The edge connects the elements j -th variable nodes and i -th check nodes only if a '1' is present in a parity check matrix H in position (i, j) [3], [79]. Tanner graph in Figure 1 is a bipartite, check node $C1$ connects to variable nodes $B1, B3$, and $B6$.

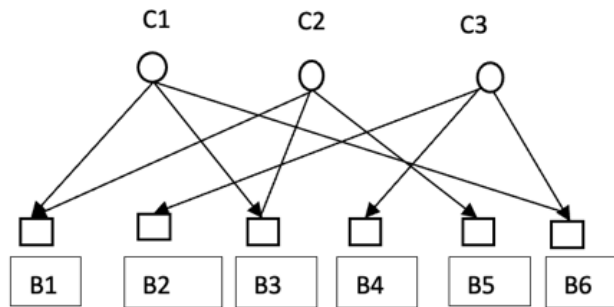


Figure 3 - 1: Tanner graph of parity check matrix H

Decoding of LDPC codes uses message-passing algorithms. In this paper, we will focus on belief propagation decoding, as presented by Gallager [81], but we will also compare it to layered belief propagation, normal min-sum, and offset min-sum. The decoder uses Log-

Likelihood Ratios (LLRs), which are updated on each iteration until the process is complete. Layered belief propagation decoding, which is based on the paper presented by Hocevar [82] performs even better than original belief propagation. The decoding process takes place by iteratively looping over subsets of rows (layers). This algorithm is faster compared to belief propagation. Chen [5] presented normalized min-sum decoding and layered min-sum decoding, which involve modifications to the equation used in layered belief propagation decoding.

This literature review examines various LDPC decoding techniques, including iterative decoding, belief propagation, layered decoding, and the min-sum algorithm. These decoding techniques have been implemented in this study because the literature demonstrates that these algorithms outperform hard decision algorithms. The algorithms are presented in section 3.2.1.1 below. The literature also explores the use of neural networks for LDPC decoding and emphasizes the effectiveness of hybrid approaches that combine different techniques. This is an exciting aspect to consider in our subsequent study, it is not directly relevant to this study. LDPC decoding can be categorized as soft or hard decision, with soft decision methods offering superior error correction but with increased complexity. The iterative decoding process involves message-passing algorithms, and several variants, such as the normalized min-sum and offset min-sum algorithms, are discussed; these have been implemented in this design. The offset min-sum algorithm is highlighted as a method that simplifies computation while maintaining decoding performance.

3.2.1.1 Algorithms of LDPC Decoders used in the System

- The algorithm 3.1: Belief Propagation LDPC Decoding [24].

Input:

H : parity-check matrix

y : received codeword

Output:

x : decoded codeword

Initialization:

Set all entries of the messages (i.e., the variable-to-check and check-to-variable messages) to some initial value (e.g., all 1s or all 0s).

While not converged:

For each variable node v , update its outgoing messages to the connected check nodes:

Compute the product of the incoming messages from all connected check nodes except the current one.

Update the outgoing message to the current check node by computing the sign of the product times the received symbol (y_v).

For each check node c , update its outgoing messages to the connected variable nodes:

Compute the sum of the incoming messages from all connected variable nodes.

Update the outgoing message to the current variable node by setting it to the sign of the sum.

Check for convergence:

If the maximum change in any message is below a threshold, stop iterating and output the estimated codeword x .

Decode the codeword:

For each variable node v , compute its estimated value by multiplying the incoming messages from all connected check nodes, and taking the sign.

It should be noted that the product and sum operations can be computed using log-likelihood ratios (LLRs), which are more numerically stable than the actual probabilities. In this case, the messages are represented as LLRs instead of probabilities. The product of LLRs can be computed as the sum of the individual LLRs, and the sum of LLRs can be computed using the log-sum-exp trick.

- Algorithm 3.2: Belief propagation decoding using LLRs:

Here is the mathematical algorithm for the belief propagation decoding algorithm using LLRs:

Input:

H : parity-check matrix

L : LLR vector for the received codeword

Output:

x : decoded codeword

Initialization:

Set all entries of the messages (i.e., the variable-to-check and check-to-variable messages) to some initial value (e.g., 0 for all).

While not converged:

For each variable node v , update its outgoing messages to the connected check nodes:

Compute the sum of the incoming messages from all connected check nodes except the current one.

Compute the updated outgoing message to the current check node as the sum of the computed sum and the LLR of the received symbol (L_v).

For each check node c , update its outgoing messages to the connected variable nodes:

Compute the product of the incoming messages from all connected variable nodes.

Compute the updated outgoing message to the current variable node as the difference between the computed product and the message from the current variable node.

Check for convergence:

If the maximum change in any message is below a threshold, stop iterating and output the estimated codeword x .

Decode the codeword:

For each variable node v , compute its estimated value as the sign of the sum of the incoming messages from all connected check nodes.

Mathematically, the equations of Belief Propagation, also known as the Sum-Product algorithm, can be defined as follows [6], [24], [83]-[84]:

1. Message Passing Equations:

- Message from variable node j to factor node i :

$$\mu_{ji}(x_j) = \prod_{\{k \in N(j) \setminus i\}} m_{kj}(x_j)$$

Here, $N(j)$ represents the set of factor nodes connected to variable node j , and $m_{kj}(x_j)$ denotes the message sent from factor node k to variable node j .

- Message from factor node i to variable node j :

$$\mu_{ij}(x_i) = \sum_{\{x_{\{N(i) \setminus j\}}\}} f_i(x_i, x_{\{N(i) \setminus j\}}) \prod_{\{k \in N(i) \setminus j\}} \mu_{ki}(x_i)$$

Here, $N(i)$ represents the set of variable nodes connected to factor node i , x_i , and x_j denote the values of variables i and j , respectively, $f_i(x_i, x_{\{N(i) \setminus j\}})$ represents the factor function associated with factor node i , and $\mu_{ki}(x_i)$ denotes the message sent from variable node k to factor node i .

2. Belief Update Equations:

- Belief at variable node j :

$$b_j(x_j) \propto \psi_j(x_j) \prod_{\{i \in N(j)\}} \mu_{ji}(x_j)$$

Here, $\psi_j(x_j)$ represents the prior distribution or observation evidence associated with variable node j .

- Belief at factor node i :

$$b_i(x_i) \propto f_i(x_i, x_{\{N(i)\}}) \prod_{\{j \in N(i)\}} \mu_{ij}(x_i)$$

Here, $x_{\{N(i)\}}$ denotes the values of variables connected to factor node i .

These equations form the foundation of the Belief Propagation algorithm, which is widely used for inference and decoding tasks in graphical models, including LDPC codes. By

iteratively updating the messages and beliefs based on these equations, the algorithm aims to converge to the most probable solution or estimate of the variables in the graphical model.

▪ Algorithm 3.3: Layered Belief LDPC decoding [85].

The LDPC decoding problem is to recover the original message from a received noisy codeword transmitted over a noisy channel. The LBP algorithm is an iterative algorithm that uses a factor graph representation of the code to propagate beliefs between variable nodes and check nodes until convergence is achieved.

Input: A parity check matrix H , a received vector y , and a maximum number of iterations T .

Step 1: Initialize the belief vectors for variable nodes and check nodes:

- a. For each variable node i , initialize the belief vector $bi(yi)$ to the likelihood function based on the received signal yi , i.e., $bi(yi) = P(yi | xi)$ where xi is the transmitted bit.
- b. For each check node j , initialize the belief vector $bj(xj)$ to the uniform distribution, i.e., $bj(xj) = 1/2$ for $xj = 0$ or 1 .

Step 2: For $t = 1$ to T :

a. Perform message passing from variable nodes to check nodes:

- i. For each variable node i , compute the outgoing messages $mi,j(xj)$ to its adjacent check nodes j using the current beliefs of all other nodes except j , i.e.,

$$mi,j(xj) = \prod_{k \neq j} bj,k(xk) / bi(xj)$$

- ii. Normalize the outgoing messages, i.e., $mi,j(xj) = mi,j(xj) / \sum_{\{xj\}} mi,j(xj)$

b. Perform message passing from check nodes to variable nodes:

- i. For each check node j , compute the outgoing messages $mj,i(xj)$ to its adjacent variable nodes i using the current beliefs of all other nodes except i , i.e.,

$$mj,i(xj) = \prod_{k \in N(j) \setminus \{i\}} mi,k,j(xj)$$

- ii. Update the beliefs of the variable nodes based on the incoming messages from the check nodes, i.e.,

$$bi(xi) = \text{prod}_{\{j \text{ in } N(i)\}} mj,i(xj)$$

iii. Normalize the beliefs, i.e., $bi(x) = bi(x) / \text{sum}_{\{x\}} bi(x)$

If the decoding threshold is reached, return the estimated codeword. Otherwise, go back to step 2.

- Algorithm 3.4: LDPC decoding, Normalised Min-Sum Propagation [86].

Step 1: Initialization: Initialize the message passing algorithm by setting all the messages from variable nodes to check nodes and from check nodes to variable nodes to 0.

Step 2: Message update from variable nodes to check nodes: For each variable node, compute and update the messages sent to its connected check nodes using the following formula:

$$m_{\{i \rightarrow j\}} = \text{sign}(c_{\{i\}}) * \tanh(|c_{\{i\}}|/2) / \text{prod}_{\{k \in N(i) \setminus \{j\}\}} (1 - \text{sign}(m_{\{k \rightarrow i\}}) * \tanh(|m_{\{k \rightarrow i\}}|/2))$$

where $m_{\{i \rightarrow j\}}$ is the message from variable node i to check node j , $c_{\{i\}}$ is the received channel output for variable node i , $N(i)$ is the set of check nodes connected to variable node i , and $\text{sign}(x)$ returns the sign of x (+1 or -1).

Step 3: Message update from check nodes to variable nodes: For each check node, compute and update the messages sent to its connected variable nodes using the following formula:

$$m_{\{j \rightarrow i\}} = 2 * \tanh(0.5 * \text{prod}_{\{l \in N(j) \setminus \{i\}\}} \tanh^{-1}(m_{\{l \rightarrow j\}}))$$

where $m_{\{j \rightarrow i\}}$ is the message from check node j to variable node i , $N(j)$ is the set of variable nodes connected to check node j .

Step 4: Message normalization: After each message update step, normalize the messages by dividing each message by the sum of its absolute values:

$$m_{\{i \rightarrow j\}} = m_{\{i \rightarrow j\}} / \text{sum}_{\{k \in N(i)\}} |m_{\{i \rightarrow k\}}|$$

$$m_{\{j \rightarrow i\}} = m_{\{j \rightarrow i\}} / \text{sum}_{\{l \in N(j)\}} |m_{\{l \rightarrow j\}}|$$

Step 5: Check for convergence: Check if the decoding has converged by comparing the received codeword with the decoded codeword. If the difference is less than a predefined

threshold, the decoding is considered successful. Otherwise, repeat steps 2-4 until convergence is achieved.

Output: Once the decoding has converged, output the decoded codeword.

In step 2, $\tanh(x)$ is the hyperbolic tangent function, and $\tanh^{-1}(x)$ is its inverse.

- Algorithm 2.7: Offset Min-Sum LDPC decoding [5].

Mathematically, the Offset Min-Sum algorithm is defined as follows:

Offset Min-Sum Algorithm (A Min-Sum Variation):

1. Initialization:

- Set all variable-to-check node messages (v-messages) to zero or some initial values.
- Set all check-to-variable node messages (c-messages) to the received channel log-likelihood ratios.

2. Message Update (Iterations): Repeat the following steps until convergence or for a predetermined number of iterations:

Variable-to-Check Update: For each variable node v connected to check node c :

- Compute the updated v -message as follows: $v_message_{v \rightarrow c} = \lambda \times \text{sign}(L_v) * \min(|L_v| + \mu, T)$

Check-to-Variable Update: For each check node c connected to variable node v :

- Compute the updated c -message as follows: $c_message_{c \rightarrow v} = \alpha \times (\sum_{\{v' \in V(c) \setminus v\}} \text{sign}(v_message_{v' \rightarrow c}) * \min(\gamma, |v_message_{v' \rightarrow c}|))$

Convergence Check:

- Check the convergence condition, similar to other decoding algorithms.

Hard Decision:

- After decoding, compare the final v -messages ($v_message_{v \rightarrow c}$) to a threshold τ and make hard decisions.

Mathematical Equations:

- Variable-to-Check Update: $v_message_{v \rightarrow c} = \lambda \times sign(L_v) * min(|L_v| + \mu, T)$

- Check-to-Variable Update: $c_message_{c \rightarrow v} = \alpha \times (\sum_{\{v' \in V(c) \setminus v\}} sign(v_message_{v' \rightarrow c}) * min(\gamma, |v_message_{v' \rightarrow c}|))$

Variables and Parameters used above are defined below in the context of an Offset Min-Sum algorithm.

N : The number of variable nodes in the LDPC code, representing bits.

M : The number of check nodes in the LDPC code, representing parity checks.

L_v : The received channel log-likelihood ratio (LLR) for variable node v . It represents the reliability of the received bit from the channel, which can be positive or negative depending on the likelihood of being a 0 or 1.

L_c : The message from check node c to variable node v . It represents the accumulated information from neighboring variable nodes.

T : A scaling factor for variable-to-check node messages. It is used to control the message values during the decoding process.

α : A scaling factor for check-to-variable node messages. It is used to control the message values during the decoding process.

γ : A threshold for check-to-variable node messages. It ensures that the message values are bounded during the decoding process.

λ : A scaling factor specific to the "Offset Min-Sum" algorithm. It is used in the variable-to-check update equation.

μ : An offset specific to the "Offset Min-Sum" algorithm. It is used in the variable-to-check update equation.

Equations:

Variable-to-Check Update ($v_message_{v \rightarrow c}$): $v_message_{v \rightarrow c} = \lambda \times sign(L_v) * min(|L_v| + \mu, T)$

Check-to-Variable Update ($c_message_{c \rightarrow v}$): $c_message_{c \rightarrow v} = \alpha \times (\sum_{\{v' \in V(c) \setminus v\}} sign(v_message_{v' \rightarrow c}) * min(\gamma, |v_message_{v' \rightarrow c}|))$

These parameters and equations are used in the context of LDPC decoding algorithms to iteratively exchange messages between variable nodes and check nodes, aiming to decode the transmitted data accurately by reducing errors in the received signal. The specific values of scaling factors (T , α , γ , λ , μ) can be determined based on the LDPC code design and the characteristics of the communication channel.

3.2.2 Adaptive Modulation

The purpose of adaptive modulation is to provide the best compromise among various factors, including robustness against transmission errors, spectral efficiency, and power consumption for both mobile and fixed users. [87]. The Modulation and Coding System (MCS) to be used for the next transmission at the transmitter is SNR, which is the ratio between the received signal and the noise power. The received signal is described by equation 3.7.

$$R_n = H_n \cdot X_n + W_n \quad (3.7)$$

H_n is the channel coefficient for any OFDM subcarrier from S_0 to S_n , X_n is the transmitted signal, and W_n is the Additive White Gaussian Noise (AWGN). The SNR is measured as follows based on equation (3.7).

$$SNR_n = \frac{H_n^2}{N_o} \quad (3.8)$$

N_o is the noise variance.

We applied the same principle but used it with LDPC codes and LLRs received from the QAM signal.

3.2.3 The f-OFDM

Many studies have been conducted to address the issue with basic OFDM, which is signal clipping. The authors in [75] have addressed this problem by proposing f-OFDM, which they term the new waveform for future wireless systems. The basic principle of OFDM is as follows, the modulator generates M subcarriers based on an assigned block corresponding to the assigned number N total consecutive subcarriers in a sequence of OFDM symbols. During an OFDM symbol, the transmitter obtains length N inverse of M new "data symbol" together with a Cyclic Prefix (CP), $N > M$ is the FFT size of the system. Mathematically, the transmitter obtains [75].

$$s(n) = \sum_{l=0}^{L-1} s_l(n - l(N + N_g)) \quad (3.9)$$

with

$$s_l(n) \triangleq \sum_{m=m'}^{m'+M-1} d_{l,m} e^{j2\pi mn/N} \text{ for } -N_g \leq n \leq N, \quad (3.10)$$

where N_g is the CP length, $d_{l,m}$ is the data symbol on subcarrier m of OFDM symbols l , L is the number of OFDM symbols, and $\{m', m' + 1, \dots, m' + M - 1\}$ is the assigned subcarrier range. The f-OFDM signal is obtained by passing the signal $s(n)$ through a well-designed spectrum shaping filter of equation (11) [75].

$$\tilde{s}(n) = s(n) * f(n) \quad (3.11)$$

$f(n)$, is the spectrum shaping filter centered in frequency at the assigned subcarriers, its bandwidth is equal to the total frequency width of assigned subcarriers, and the time duration is a portion of an OFDM symbol duration thus making it a perfect filter. At the receiver, the signal is passed through a matched filter $f*(-n)$, thereafter, the signal is passed through a regular OFDM receiver which removes the CP. The FFT process is applied and OFDM symbols are extracted and passed through a demodulator. It should be noted that $f(n) * h(n) * f*(-n)$ is estimated and equalized by the equalization block.

3.2.4 The Channel Model

Ka-band satellite channel is affected by weather impairments, mainly it is the fading or attenuation due to rain since the Ka-band (26.5 - 30) GHz has a very short wavelength i.e., the wavelength is slightly over 7.5 millimeters as described by the basic equation (3.12)

$$\lambda = \frac{v}{f} \quad (3.12)$$

A digital modulated signal $s(t)$ is transmitted over the channel then, the real part of the transmitted signal is described by equation (3.13) [3].

$$s(t) = \text{Re}[s'(t)\exp(j2\pi f_c t)] \quad (3.13)$$

where $s'(t)$ is the equivalent lowpass transmitted baseband signal of $s(t)$ in the time domain, the equivalent lowpass received signal is given by equation (3.14) [3].

$$r(t) = \int_{-\infty}^{\infty} C(f, t) S'(f) \exp(j2\pi f_c t) df + n(t) \quad (3.14)$$

$C(f, t)$ is the Ka-band channel multiplicative fading process, since the Ka-band satellite communication channel is a slow frequency nonselective fading channel, it changes slowly with time. $C(f, t)$ can be regarded as a complex-valued constant for at least one symbol interval. Let $C(f, t) = A \exp(j\emptyset)$ [3]. Substituting into equation (3.14) we get equation (3.15) [3].

$$r(t) = \int_{-\infty}^{\infty} A \exp(j\emptyset) S'(f) \exp(j2\pi f_c t) df + n(t)$$

$$= A \exp(j\emptyset) s'(t) + n(t) \quad 0 \leq t \leq T \quad (3.15)$$

where A and \emptyset are equivalent lowpass envelope and phase respectively, they are random processes. T is the time duration of the modulated symbol and $n(t)$ is the AWGN.

3.2.4.1 The Fixed Satellite Channel

The fixed satellite channel signal envelope and signal phase can be modeled as a Gaussian distribution, which incorporates the fading caused by weather conditions. This is based on the extended Loo's model, as referred to in the literature in Chapter 2.7. The Probability Density Function (PDF) of the signal envelope A and the signal phase \emptyset can be described in terms of statistical models [3]. The PDF of the envelope and phase are given by equations (16) and (17) respectively [4].

$$p(A) = \left(\frac{1}{\sqrt{2\pi\sigma'^2}} \right) \exp \left[\frac{-(A-m')^2}{2\sigma'^2} \right] \quad (3.16)$$

$$p(\emptyset) = \left(\frac{1}{\sqrt{2\pi\sigma''^2}} \right) \exp \left[\frac{-(\emptyset-m'')^2}{2\sigma''^2} \right] \quad (3.17)$$

m' and m'' are the mean value of the signal envelope and phase respectively, σ' and σ'' are the signal envelope and phase variance [4]. Authors in [4] have used extended Loo's model to build the rain fade channel. The mean and variance values for different weather conditions are given in Table 3-1 and Table 3-2. The statistical immovable Ka-band satellite communication model is shown in Figure 3-2 [4].

Table 3 - 2: Immovable Ka-band satellite weather envelope attenuation measurements [4].

Weather conditions	m'	σ'^2
Sunny	0.455	0.00056
Light snow	0.499	0.00022
Moderate Rain	0.662	0.02
Thunderstorm	0.436	0.01386

Table 3 - 3: Immovable Ka-band satellite weather phase attenuation measurements [4].

Weather conditions	m''	σ''^2
Sunny	0.0079	0.00381
Light snow	0.0499	0.00022
Moderate Rain	-0.0089	0.03077
Thunderstorm	0.0068	0.00414

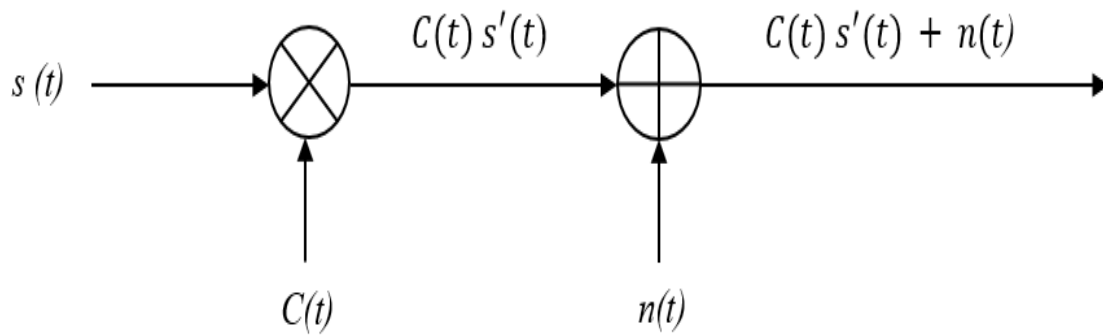


Figure 3 - 2: The statistical immovable Ka-band satellite communication model [4].

3.2.4.2 Land Mobile Satellite (LMS) Channel

The multipath and shadowing can be modeled as Rayleigh and Rician fading [3]-[4], the radio signals arriving at the received via multipath with no line of site are Rayleigh distribution and the radion signals with the strong Line Of Site (LOS) are Rician distribution. The multipath and shadowing can be modeled as Rayleigh and Rician fading [3]-[4], the radio signals arriving at the received via multipath with no line of site are Rayleigh distribution. The Rayleigh PDF of the signal envelope y is given by equation 3.18.

$$p(\gamma) = \left(\frac{\gamma}{2\pi\sigma'}\right) \exp\left[\frac{-\gamma^2}{2\sigma'^2}\right] \quad (3.18)$$

Where σ' represents the variance, as described by equation 3.16.

Some radio waves encounter obstacles such as buildings, trees, which cause attenuation known as shadowing. The received signal envelope β PDF of shadowing follows a lognormal distribution, as given by the following equation.

$$p(\beta) = \left(\frac{1}{\sqrt{2\pi\sigma'}\beta}\right) \exp\left[\frac{-(\ln\beta - m)^2}{2\sigma'^2}\right] \quad (3.19)$$

m represent the mean as described in equation 3.16

The received LMS signal with only the surrounding fading is therefore given by

$$r_e \exp(\theta) = \beta \exp(j\phi_s) + \gamma \exp(j\phi_m) \quad (3.20)$$

$\beta \exp(j\phi_s)$ is the LOS component and $\gamma \exp(j\phi_m)$ is the multipath component with β and γ from equation 3.18 and equation 3.19 respectively. The ϕ_s and ϕ_m represent the phase uniform distribution over $[0, 2\pi]$.

3.2.5 The working of the system

We propose the improved system model as compared to the system model presented in [3]. The improvement proposed is to integrate adaptive modulation and f-OFDM as discussed in the introduction, the system diagram is shown in Figure 3-3. The transmitter encodes the binary information using the LDPC encoder. The encoded information is modulated using different levels of the QAM modulator depending on the level of SNR by applying an adaptive modulation algorithm that uses switching thresholds shown in Table 3-3. Initially, the modulation order is set to $M = 16$ as system bootup; thereafter, it follows the SNR threshold table based on the SNR which is generated randomly between -10 dB and 0 dB to simulate the real transmission scenario in fading Ka-band channel. The complex modulated data is mapped into parallel and then converted from the frequency domain into the time domain by the Inverse Fast Fourier Transform (IFFT) and applied to the matched filter

thereafter, the system adds the cyclic prefix, converted from parallel to serial, and transmitted into the channel.

The receiver process is the opposite, it converts data from serial to parallel, applies a matched filter on the received signal, and transforms the signal from the time domain to the frequency domain by using the Fast Fourier Transform (FFT). The signal is converted from serial to parallel and demodulated based on the received SNR level as per the adaptive modulation threshold Table. Demodulated complex data is decoded by the LDPC decoder and the transmitted data is recovered with very less errors. The information about the instantaneous level of the SNR is fed back to the transmitter via the feedback channel, the receiver then reconfigures the modulation level for the next transmission. The transmitter also reconfigures the modulation based on the feedback information received from the receiver so that the receiver and the transmitter are aligned. The channel estimation is assumed at the receiver.

3.2.5.1 Integration of Adaptive Modulation and f-OFDM

The adaptive modulation algorithm monitors the instantaneous SNR received f- OFDM. Integrating adaptive modulation and f-OFDM creates a system that dynamically optimizes both the modulation scheme and the spectral characteristics of the signal to adapt to changing channel conditions. This results in improved data throughput, spectral efficiency, and reliability in wireless communication systems, especially in scenarios with varying interference or noise levels. The f-OFDM and adaptive algorithm have been implemented in Matlab as follows: The filtering is applied in the frequency domain signal after the IFFT has converted the modulated data into a time-domain signal. The purpose of this filtering is to shape the spectral characteristics of the OFDM signal, reducing out-of-band emissions and improving spectral efficiency. This occurs before the signal is transmitted and before adding the cyclic prefix (CP). At the receiver, the filtered received signal is demodulated back to the frequency domain using the FFT, and afterward, we apply the adaptive modulation as explained above.

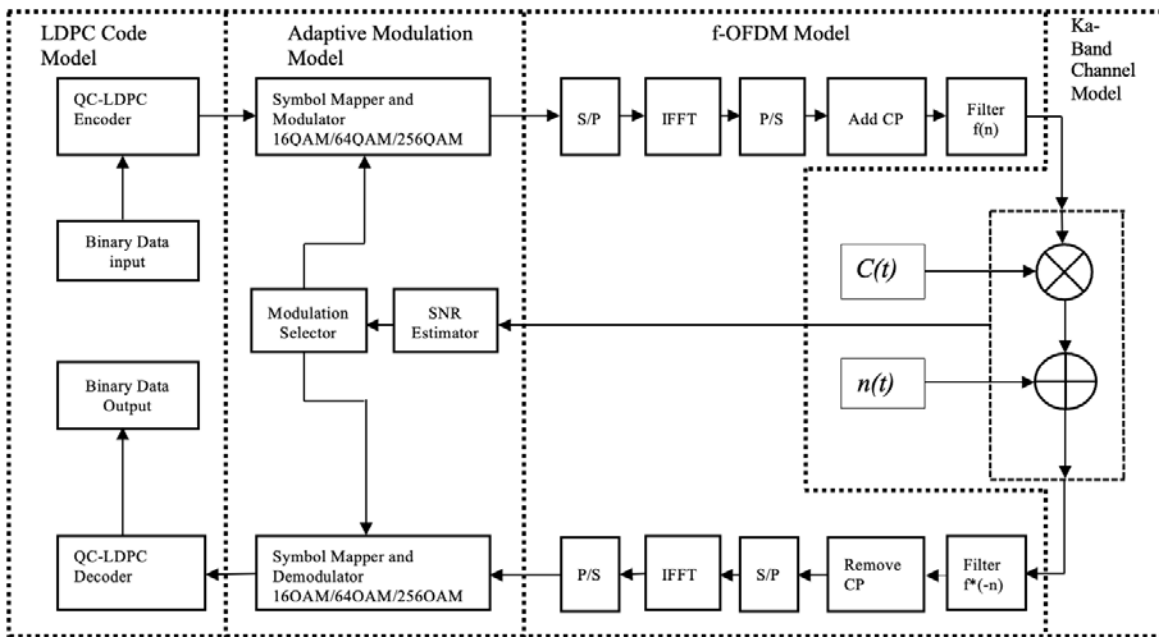


Figure 3 - 3: Block diagram of the system with LDPC codes, adaptive modulation, f-OFDM and the fixed Ka-band channel model.

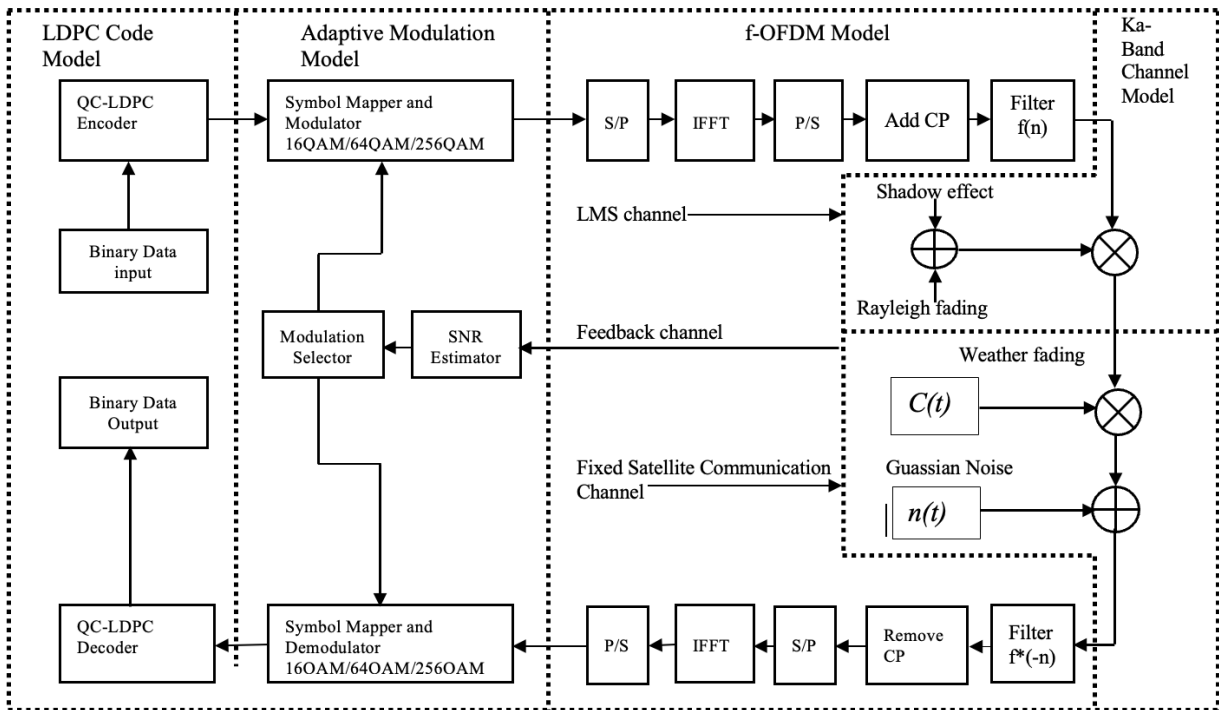


Figure 3 - 4: Block diagram of the system with LDPC codes, adaptive modulation, f-OFDM, LMS and the Fixed Ka-Band Satellite Channel.

3.2.5.1 Optimizing Ka-Band Satellite Communication: Dynamic

Adaptive Modulation and LDPC Coding

Please refer to Table 3-3 below, in the challenging context of Ka-band satellite communication, particularly during adverse weather conditions like rain, stringent thresholds for adaptive modulation are crucial. These thresholds, based on a dynamic evolution model accounting for temporal variations in channel conditions, ensure reliable communication by dynamically adjusting modulation schemes. By optimizing spectral efficiency and balancing data rate with reliability, this approach enhances system performance, enabling seamless communication despite the evolving nature of the channel over time. However, it's important to note that the term "AMC" may be inaccurate in this context, as the LDPC code rate remains constant while only the adaptive modulation changes. The LDPC code rate, being a powerful coding technique, remains unchanged, though future researchers could explore varying the LDPC coding rate for further optimization.

Table 3 - 4 Switching threshold for M-QAM SNR-based adaptive modulation algorithm.

Mode	QAM Modulation Order	Thresholds
1	16	$-10 \leq \text{SNR} \leq -7$
2	64	$-7 < \text{SNR} \leq -4$
3	256	$\text{SNR} > -4$

3.2.6 The Summary

Chapter 3 explores the complexities of designing future satellite communication systems operating at Ka-band frequencies, addressing challenges like rain attenuation and limited spectral efficiency. To tackle these issues, the chapter proposes integrating LDPC codes system with adaptive modulation, and f-OFDM to form one robust system. LDPC codes are extensively discussed for their role in achieving reliable communication with low BER, crucial in satellite and mobile communication systems. Various decoding algorithms, including belief propagation and the min-sum algorithm, are examined for their effectiveness in error correction.

The chapter provides a detailed system model, starting with LDPC codes and their decoding techniques. It emphasizes LDPC codes' significance in achieving robust communication and delves into decoding algorithms' intricacies. Furthermore, the introduction of f-OFDM

addresses signal clipping in basic OFDM systems by utilizing spectrum shaping filters to enhance spectral efficiency and reduce out-of-band emissions. By integrating adaptive modulation and f-OFDM, the proposed system dynamically optimizes modulation schemes and spectral characteristics based on changing channel conditions, ensuring efficient data throughput and reliability.

The integration of adaptive modulation and f-OFDM into the system model presents a dynamic approach to optimize modulation schemes and spectral characteristics based on instantaneous SNR levels. This dynamic optimization enhances data throughput, spectral efficiency, and reliability in the Ka-band satellite communications. By implementing these components in MATLAB and conducting meticulous analysis, the chapter effectively bridges the gap between system modeling and design objectives, providing a robust foundation for subsequent simulations and evaluations of future satellite communication systems.

CHAPTER FOUR

Simulations and Results Discussion

4.1 Introduction

The simulation was conducted using the Matlab 2022R2 package. The mathematics discussed above were carefully translated into Matlab coding, ensuring that we used appropriate parameters, as shown in Table 4-1. We took advantage of Matlab's built-in simulation toolboxes, which simplified the code length. The parameters shown in Table 4-1 were chosen based on the following criteria.

4.2 The System Simulation

The simulation parameters shown in Table 4-1 were chosen based on the following criteria.

4.2.1 LDPC Code Parameters

- Parity Check Matrix (H): We used Quasi-cyclic LDPC codes are often chosen due to their regular structure and good error-correcting performance.
- Parity Check Matrix Block Size: We chose the block size of 27 to provide better error correction performance.
- Row Weight and Column Weight: A row weight of 6 and a column weight of 24 indicate the distribution of 1s in the parity check matrix. This choice is based on the trade-off between error correction performance and complexity.
- LDPC Code Rate: A code rate of $3/4$ is chosen, this is a common rate for LDPC codes in many communication standards and to make the coding simpler, we used a Matlab built-in function with a code rate of $3/7$.

4.2.2 LDPC Encoder and Decoders

- LDPC Encoder: The choice of using a Quasi-Cyclic encoder based on IEEE 802.11 standards was chosen to make our system compatible with widely adopted communication standards, and of course for performance consideration.
- LDPC Decoders: Belief Propagation, Layered Belief, Normalized Min-Sum, and Offset-Min Sum are common decoding algorithms for LDPC codes, offering a range of trade-offs between performance and complexity. We chose these as they are known to perform better as indicated by the literature review.

- Decoding Iterations: 10 decoding iterations specified which is a reasonable choice to balance performance and computational complexity.

4.2.3 Modulator and OFDM Parameters

- Number of OFDM Subcarriers: 2048 subcarriers are chosen for high-data-rate communication systems.
- OFDM Cyclic Prefix: A cyclic prefix of 16 samples is specified to mitigate inter-symbol interference.
- OFDM Filter Length: A long filter length of 513 was chosen to control spectral properties and provide good performance in the presence of multipath channels.
- OFDM Filter Tone Offset: A tone offset of 25.5 is used for control and compatibility with the selected system parameters.
- Modulator: The choice of modulation schemes ranging from M=16 to M=256 provides flexibility for adapting to different channel conditions and data rates.
- Eb/No: The chosen range of -10 dB to 0 dB allows for a wide range of signal-to-noise ratios to assess system performance.
- Adaptive Modulation Type: SNR-based adaptive modulation is employed to optimize data rates under varying channel conditions.

4.2.3 Channel Parameters:

- Eb/No Range: The specified Eb/No range covers a variety of signal-to-noise ratios that allow you to analyze system performance under different noise conditions.
- Default System Noise: The use of AWGN (Additive White Gaussian Noise) is necessary for simulating channel noise in theoretical analyses, we are referring to the system thermal noise of the components therefore, AWGN is necessary on all systems.
- Ka-band Fading Channel: The Gaussian distribution model with multiplicative noise is chosen to simulate real-world channel characteristics of a fixed Ka-band channel model. Weather Conditions including different weather conditions (Sunny, Thunderstorm, Light Snow, Moderate Rain) allows for assessing the impact of environmental factors and allows us to test the system's performance. The simulated model is that of a fixed Ka band channel.

4.2.4 Simulation Stopping Criteria:

In the simulation context, the number of errors and the number of bits serve as critical parameters, setting thresholds for the number of errors and transmitted bits, respectively. These thresholds play a pivotal role in determining when to halt the simulation process, ensuring that we gather an adequate amount of data to conduct thorough and meaningful performance assessments. By establishing predefined thresholds for errors and transmitted bits, we can effectively monitor the simulation's progress and terminate it once a sufficient amount of data has been collected. This approach enables us to strike a balance between computational efficiency and the accuracy of our results, allowing us to draw robust conclusions regarding the system's performance under various conditions.

4.1 Matlab Simulation Parameters

Table 4 - 1: LDPC Parameters

Parity check matrix (H)	Quasi Cyclic
Parity check matrix block size	27
Row weight and column weight	6, 24
LDPC code rate	3 / 4
LDPC encoder	Quasi Cyclic, IEEE 802.11 standards
LDPC decoders	Belief Propagation, Layered Belief, Normalised Min-Sum, and Offset-Min Sum
Decoding iterations	10

Table 4 – 2: Modulator and OFDM Parameters

Number of OFDM subcarriers	2048
OFDM cyclic prefix	16
OFDM filter length	513
OFDM filter tone offset	25.5
Modulator	M = 16, M = 64 and M = 256
Adaptive modulation type	SNR-based adaptive modulation (SNR threshold feedback)

Table 4 - 3: Channel Parameters

Eb/No Range	-10 dB to 0 dB
Default System Noise	AWGN
Ka-band Fading Channel	Gaussian distribution Model : Multiplicative Noise
Weather conditions	Sunny, Thunderstorm, Light Snow, Moderate Rain
Simulation stopping criteria	NumErrs < 2000 && NumBits < 1e7

4.2 Results Discussion

In this section, we delve into the analysis and interpretation of the results obtained from our experiments. We examine the key findings and trends observed during the simulations, providing insights into the performance and behavior of the system under various conditions. By scrutinizing the data and comparing it with theoretical expectations, we aim to elucidate the implications of our findings and their significance in the context of the broader research objectives. Through a comprehensive discussion, we seek to uncover underlying patterns, address research questions, and offer valuable insights for future studies and practical applications.

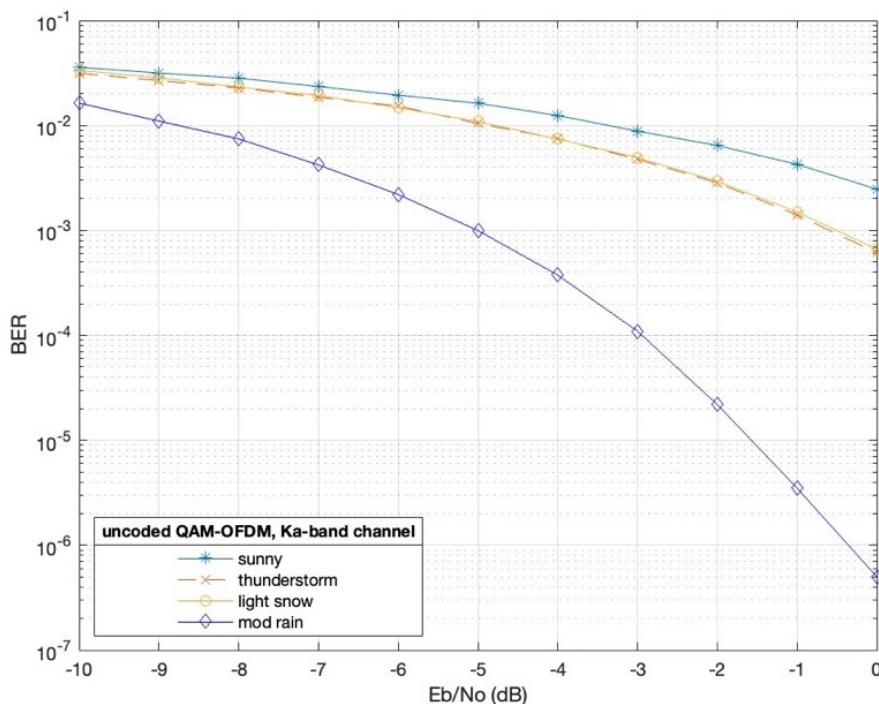


Figure 4 - 1: Uncoded 16-QAM - OFDM under all Ka-band weather scenarios

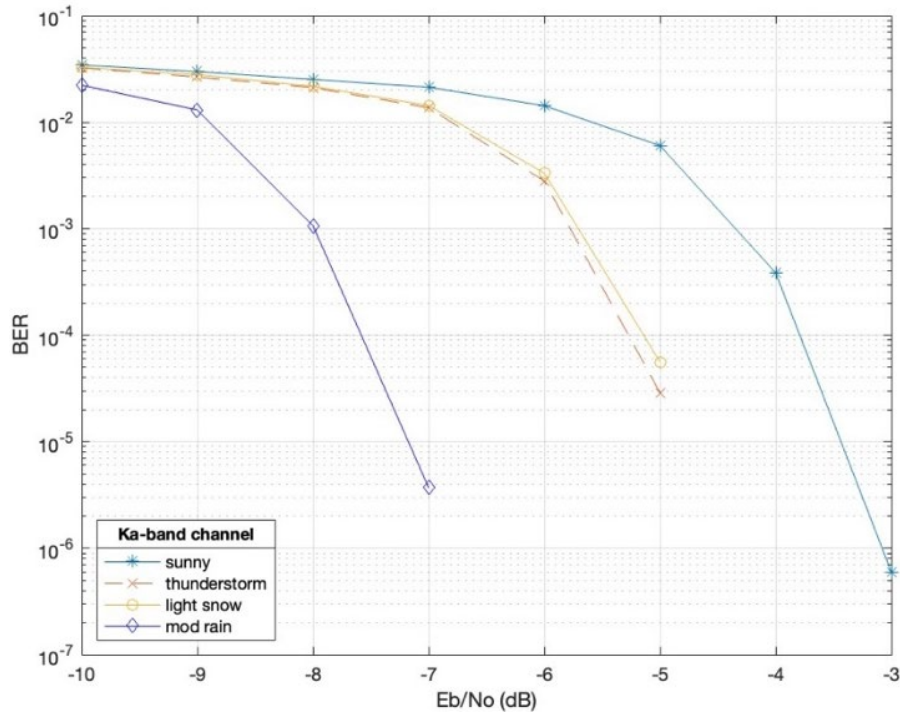


Figure 4 - 2: 16-QAM - OFDM LDPC coded under all Ka-band weather scenarios

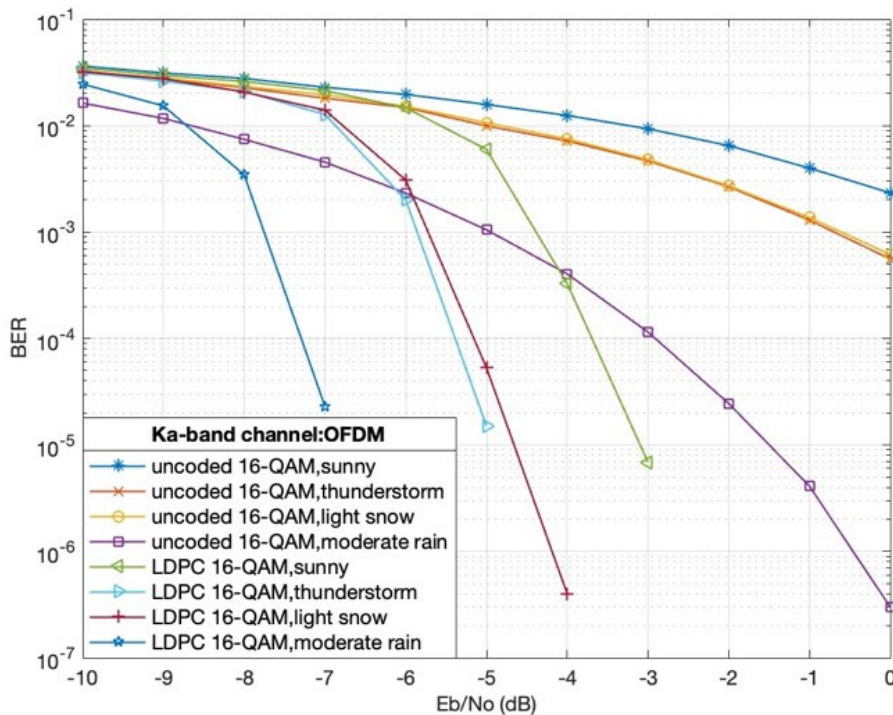


Figure 4 - 3: Uncoded 16-QAM-OFDM vs LDPC coded 16-QAM-OFDM.

Figure 4-1 demonstrates the effects of rain fading on the Ka-band satellite channel, which utilizes an uncoded 16-QAM OFDM signal. The performance has improved due to the

addition of OFDM into the system. It is noticeable that the system performs better under moderate rain weather conditions, achieving a gain of 4.3 dB compared to light snow and thunderstorm weather conditions at a BER 10^{-3} . When comparing Figure 4-1 to Figure 4-2, the effects of LDPC coded 16-QAM - OFDM signal can be observed. Examining the BER of 10^{-3} , the Eb/No is -8 dB for the LDPC coded signal, whereas the uncoded 16-QAM - OFDM signal operates at an Eb/No of -5 dB for the same BER. Therefore, the LDPC coded signal achieved a gain of 3 dB. Figure 4-3 compares the results at BER 10^{-3} against the uncoded system, yielding the following findings: LDPC-coded OFDM achieves a gain of 2.8 dB under moderate rain weather conditions, while in thunderstorm weather, the LDPC coded - OFDM system achieves a gain of 5.1 dB. LDPC codes improve the BER for light snow by attaining a gain of 5 dB. In sunny weather conditions, LDPC codes achieve a BER of 10^{-3} at 4.4 dB, while the uncoded system operates above an Eb/No of 0 dB. LDPC codes achieve a gain of above 4.4 dB in this scenario. These results prove that LDPC codes are capable of error correction in severe weather conditions.

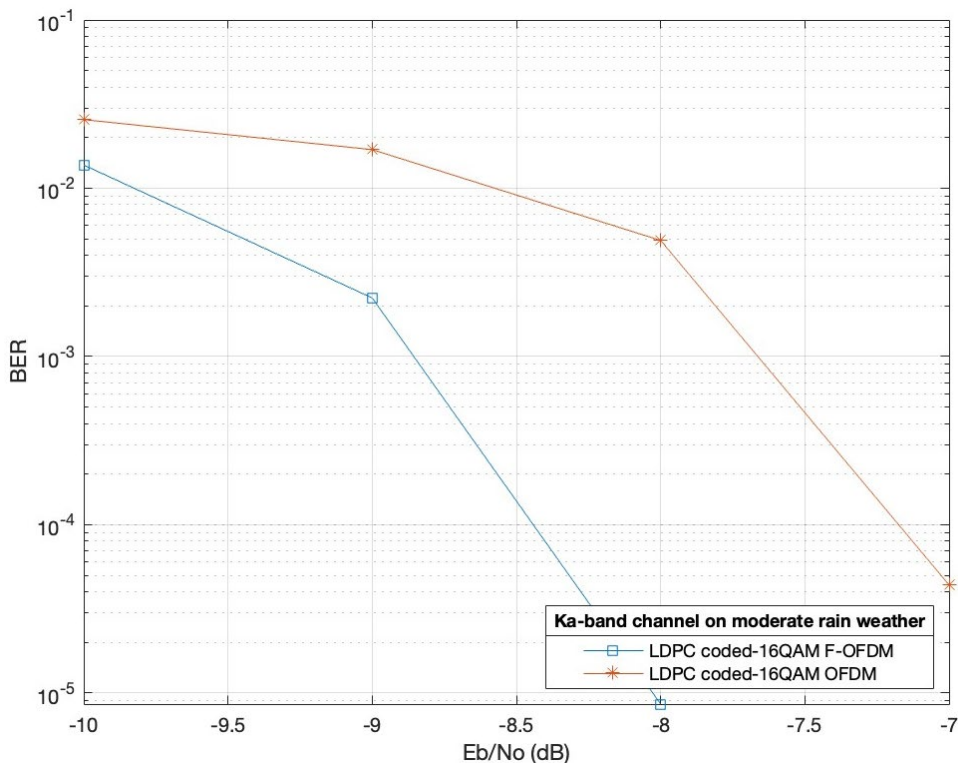


Figure 4 - 4: LDPC coded 16-QAM f-OFDM vs LDPC coded 16-QAM OFDM on moderate rain in the Ka-band satellite channel.

In Figure 4-4, we introduce the f- OFDM into LDPC-coded 16-QAM and compare it to LDPC-coded 16-QAM-OFDM. f-OFDM further improves the performance of LDPC codes.

LDPC 16-QAM f-OFDM system achieves the BER of 10^{-3} at the E_b/N_o - 8.8 dB while LDPC 16-QAM OFDM is at -7.7 dB for the same BER of 10^{-3} . The enhanced system using the f-OFDM system has achieved a gain of 1,1 dB. The introduction of f-OFDM further improves the system's performance. The results show improvement compared the reference main paper of this thesis.

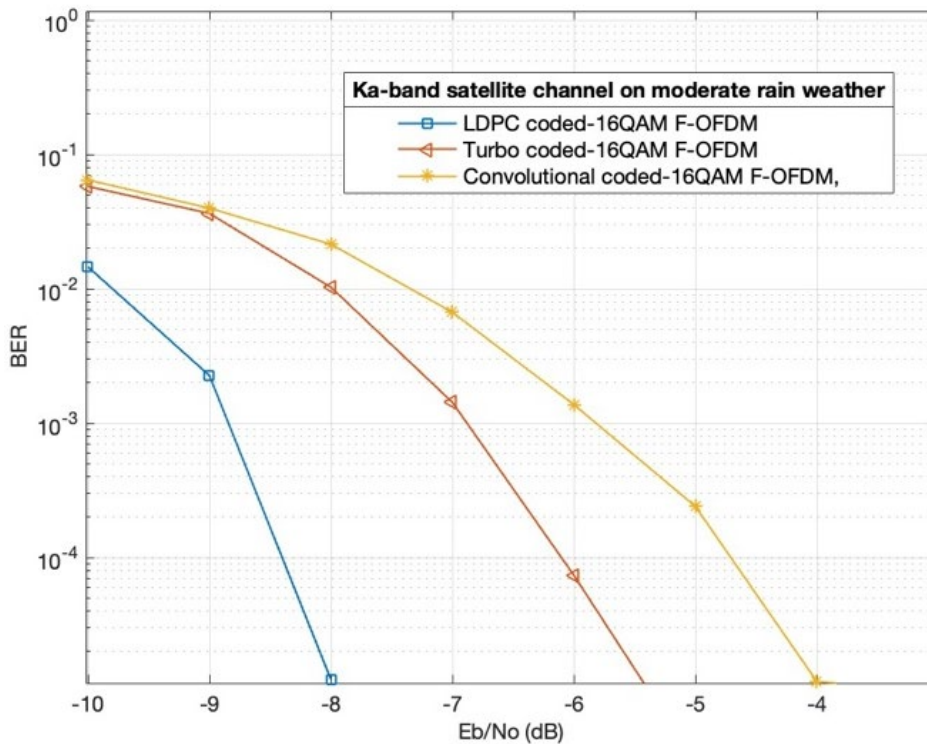


Figure 4 - 5: LDPC code 16-QAM f-OFDM vs Turbo code 16-QAM f-OFDM vs CC 16-QAM f-OFDM on moderate rain weather in the Ka-band satellite channel.

Figure 4-5 compares the performance of LDPC codes to Turbo codes and CC for the same Ka-band satellite channel, in moderate rain conditions. We apply f-OFDM to all three FEC codes to make a fair comparison. We can see that LDPC codes are still outstanding, performing better than Turbo codes and CC. LDPC codes achieve a gain of 2 dB when compared to Turbo codes at the BER of 10^{-3} and a gain of 3 dB when compared to CC at the same BER.

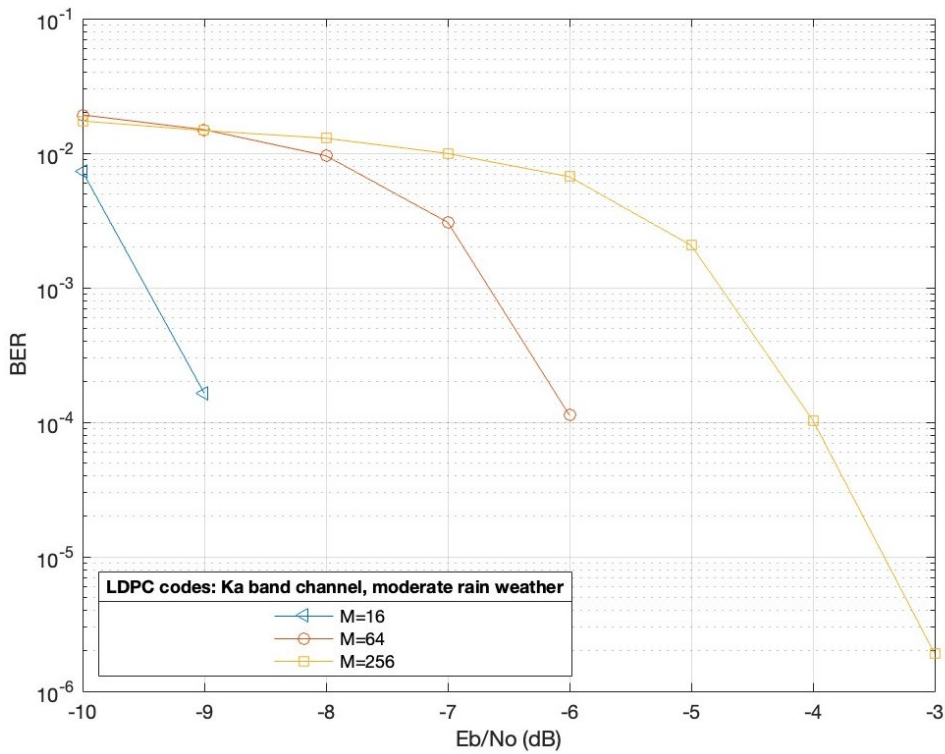


Figure 4 - 6: Simulation of different M-QAM levels

We compared different M-QAM levels in Figure 4-6 to verify that our systems can transmit more data as we increase the modulation. However, it is important to note that the BER increases with high modulation when channel conditions deteriorate. This is why we implemented adaptive modulation, as shown in Figure 4-9. We observed good performance when M is 16, comparing M = 16 to M = 256 at a BER 10^{-3} . The M-QAM level 16 achieved a gain of 4.7 dB against M = 256 and achieved a gain of 2.9 dB against M = 64.

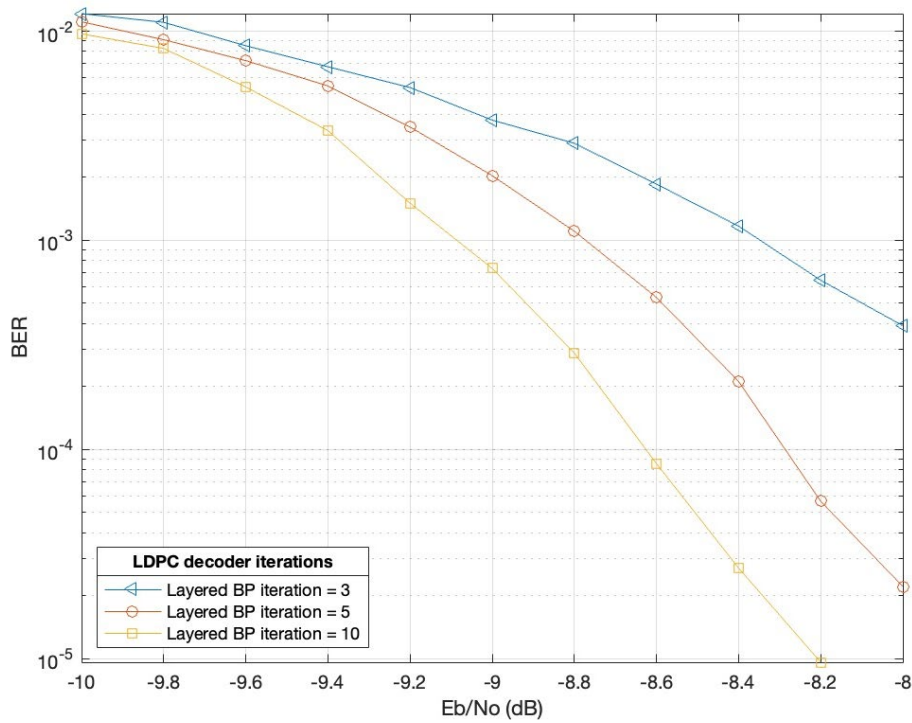


Figure 4 - 7: Comparison of LDPC decoding iterations 3, 5, and 10.

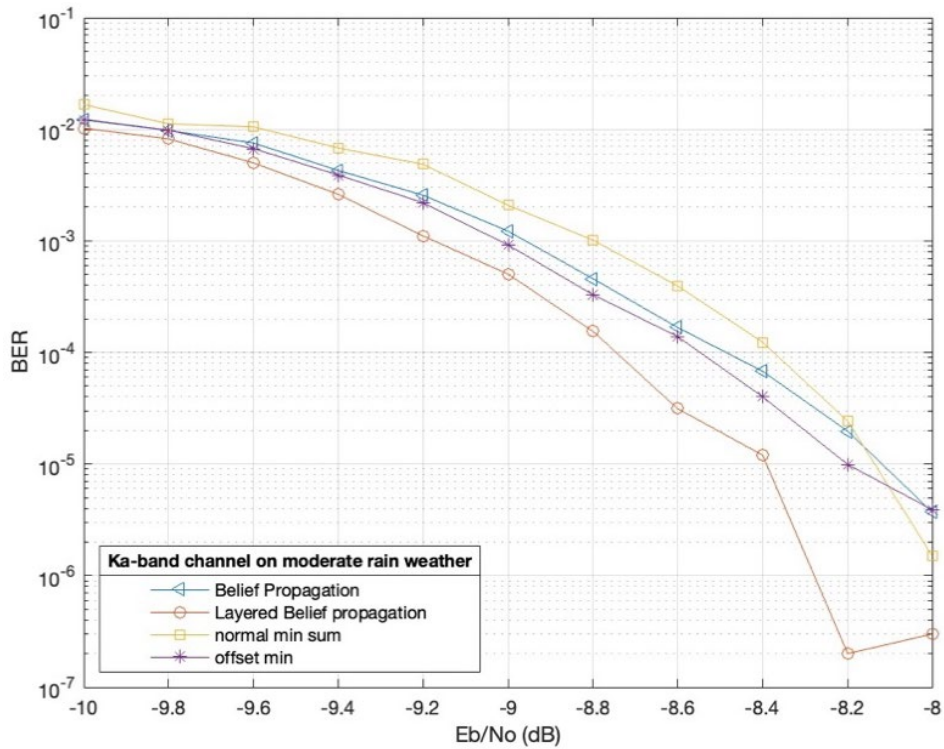


Figure 4 - 8: LDPC soft decoding algorithms comparison.

We compare the performance of the LDPC decoder iteration in Figure 4-7, we use L-BP, iterations set to 3, 5, and 10. We achieve better performance if the iteration is set to 10 as the

yellow line with square markings represents the L-BP with iterations set to 10. This addresses the computational complexity whereby we show that L-BP performs better when decoding iterations are set to 10, followed by 5 iterations, and then 3 iterations. Fig. 4-7 showed that a higher number of iterations improves performance, but it comes at the cost of more computing time. In Figure 4-8, we compare different LDPC decoding algorithms, we can see that, layered belief propagation performs better followed by offset min-sum, but layered belief propagation performance starts to degrade at E_b/n_0 8.2 dB, and at that point, normal min-sum performance starts improving. Belief propagation and normal min-sum performance are almost similar.

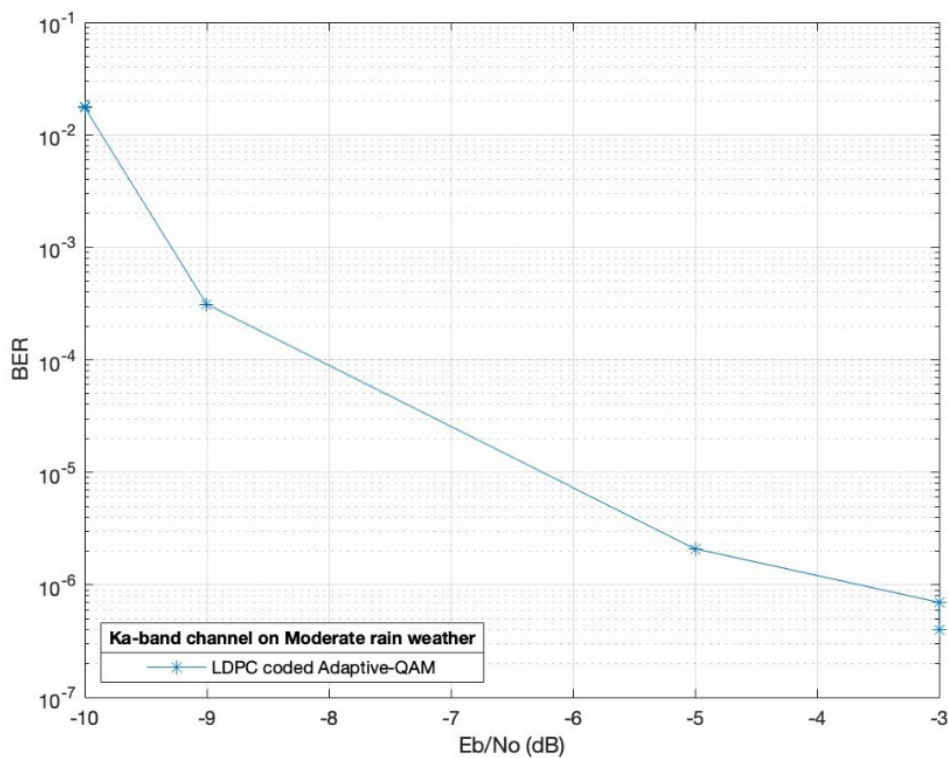


Figure 4 - 9: LDPC codes QAM f-OFDM adaptive modulation: Ka-band satellite channel on moderate weather.

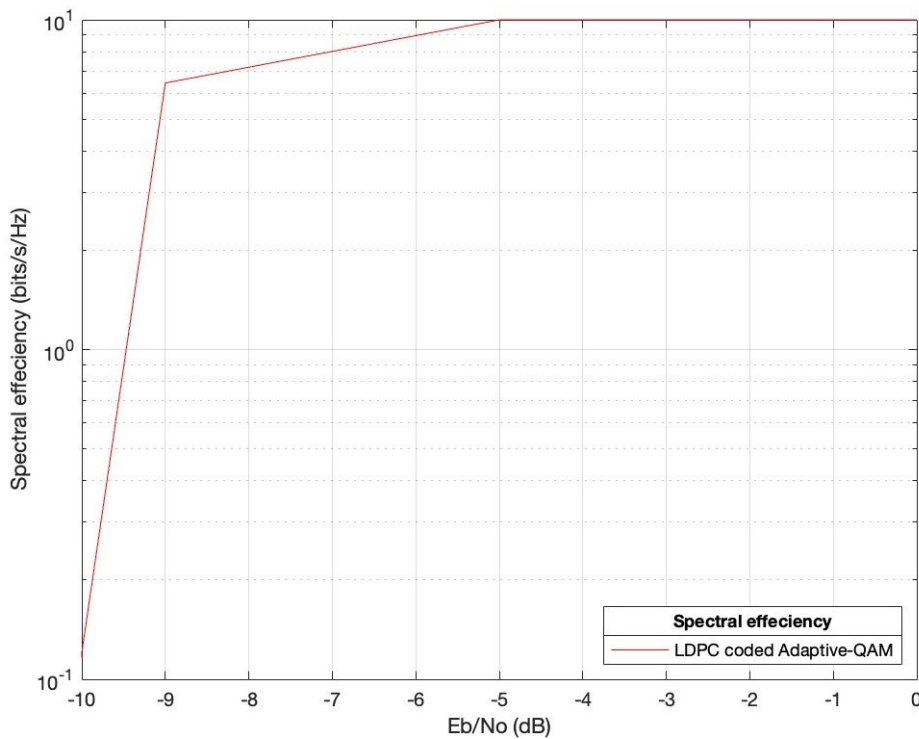


Figure 4 - 10: Spectral efficiency of LDPC codes QAM f-OFDM adaptive modulation: Ka-band satellite channel on moderate weather.

Figure 4-9 and Figure 4-10 illustrate the impact of adaptive modulation on the LDPC code system utilizing f-OFDM in the Ka-band satellite communication. In Figure 4-9, a modulation switch occurs from 16-QAM to 64-QAM at an E_b/N_0 of -9 dB. Correspondingly, Figure 14 reveals an improvement in spectral efficiency at the same E_b/N_0 of -9 dB. Furthermore, Figure 4-9 demonstrates another switch from 64-QAM to 256-QAM at an E_b/N_0 of -5 dB, resulting in an additional improvement in spectral efficiency as depicted in Figure 14. The utilization of adaptive modulation significantly enhances the system's spectral efficiency. Therefore, it can be concluded that when the E_b/N_0 is low, the system employs a lower modulation order, while it switches to a higher modulation order as signal quality improves. It's important to note that the system has been optimized and calibrated for moderate rain conditions, resulting in improved performance under those specific circumstances.

CHAPTER FIVE

Conclusion and Recommendations

5.1 Conclusion

This research has been conducted, and we have achieved our objective as planned. We can conclude as follows, starting from the literature review. The literature provided us with direction, enabling us to select the type of LDPC code suitable for the application of Ka-band multiplicative noise. While our goal was to improve the system's performance using LDPC codes, we also aimed to reduce the computing time required for LDPC encoding and decoding. According to the literature, it has been reported that RA-LDPC codes and the QC-LDPC encoder designed for IEEE 802.11n exhibit reduced encoding complexity, allowing for swift encoding processes without burdening the processors. After conducting a thorough evaluation, we have concluded that the preferred method is the QC-LDPC encoder.

Furthermore, the review of LDPC decoding has revealed that soft decision decoders tend to be more effective in error correction when compared to hard decision decoders. To explore this further, we compared four different types of LDPC decoding techniques: Belief Propagation, Layered Belief Propagation, Normalised Min Sum Algorithm, and Offset Min Sum Algorithm. The simulations have shown that Layered Belief Propagation performs better, followed by Offset Min Sum, at a very low SNR. However, Layered Belief Propagation's performance starts to degrade at high SNR. On the other hand, the performance of the Normal Min-Sum improves at high SNR, and then both Belief Propagation and Normal Min-Sum perform very closely. It's important to note that this performance cannot be generalized because it could be specific to this particular application. Nevertheless, we gain an understanding of how these SPA algorithms compare in terms of performance.

Due to the characteristics of the Ka-band channel, we chose to implement adaptive modulation. However, we needed to consult the literature for guidance and insights. The literature review guided us to the selection of SNR-based adaptive modulation as a well-informed choice. The reviewed studies have demonstrated the effectiveness and benefits of adapting the modulation scheme based on the SNR of the communication channel. This approach allows the transmitted signal to dynamically vary its modulation type and symbol rate to optimize performance in changing channel conditions. This is the reason why we selected this algorithm.

By utilizing SNR-based adaptive modulation, wireless systems can achieve improved spectral efficiency and enhanced error correction capabilities. Researchers have developed algorithms and techniques to dynamically adjust the modulation level and coding rate in real-time, maximizing system throughput while maintaining reliable communication [53]. This approach has been widely adopted in commercial wireless systems due to its ability to adapt to varying SNR levels and optimize system performance accordingly.

Overall, the literature supports the selection of SNR-based adaptive modulation as a promising strategy to improve wireless communication. It leverages the insights and methodologies from the referenced studies, providing a flexible and efficient approach to optimize the use of available resources and adapt to changing channel conditions. Eventually, we added the f-OFDM to improve the overall performance of the system as guided by the literature, the results show remarkable improvement from the previous research. After successfully conducting our research, we can conclude that the literature review played a crucial role in guiding our decisions because it helped us to select the best encoder, decide on decoders, f-OFDM, and the adaptive modulation algorithm. We selected the QC-LDPC encoder for efficient LDPC encoding and decoding while considering the benefits of soft decision decoders over hard decision decoders. Layered Belief Propagation performed best at low SNR, while Normal Min-Sum showed improvement at high SNR. The literature also supported the implementation of SNR-based adaptive modulation, which dynamically adjusts the modulation scheme and symbol rate based on channel conditions. Furthermore, the addition of f-OFDM resulted in significant performance improvements compared to previous research. The incorporation of additional layers has demonstrated significant enhancements in performance. However, it is imperative to acknowledge the accompanying drawbacks. As additional layers are introduced, computational time escalates, leading to increased latency. Hence, prudent deliberation is essential, with parallel computing emerging as a pivotal solution among various alternatives.

5.2 Recommendations

There is room for improvement in this study, and future researchers can explore the design of LDPC codes in greater detail, specifically focusing on the choice of the parity check matrix. While the QC-LDPC parity check matrix is considered the best, its design plays a crucial role in determining the overall performance. Therefore, optimizing the design of the parity check matrix has the potential to further enhance the results of the study. This study utilized SNR-based adaptive modulation. However, future researchers can explore further improvements in adaptive modulation techniques. One potential approach is the combination of SNR-based and BER-based adaptive modulation, which is expected to enhance performance due to its advantages, including improved spectral efficiency, enhanced error correction capabilities, robustness to channel variability, flexibility, adaptability, and QoS optimization in wireless communication systems.

Lastly, researchers can incorporate adaptive rate LDPC codes to complement adaptive modulation techniques. This integration has the potential to further enhance system performance by dynamically adjusting the coding rate based on the varying channel conditions. The system performs very well under rainy conditions, however, the same optimization may not be as effective for sunny weather conditions. Although performance in sunny weather has shown improvement compared to the findings in [4], it still falls short as compared to adverse weather condition's performance. While the system currently performs acceptably under sunny weather, there is room for further improvement.

REFERENCES

- [1] H. Tsuji, A. Miura, A. Carrasco-Casado and M. Toyoshima, "R&D for Satellite Communications and Non-terrestrial Networks toward Beyond-5G in Japan," *2022 27th Asia Pacific Conference on Communications (APCC)*, Jeju Island, Korea, Republic of, 2022.
- [2] G. Busuttill-Reynaud and L. J. Elliott, "A multi service mobile satellite communications system operating at Ka-band," *IEE Colloquium on Future of Ka-band for Satellite Communications*, 1993, pp. 8/1-8/7.
- [3] X. Da, Y. Wang and T. Xie, "Performance of LDPC Codes for Satellite Communication in the Ka-band," *2009 5th International Conference on Wireless Communications, Networking and Mobile Computing*, Beijing, 2009, pp. 1-4.
- [4] L. Luini and C. Capsoni, "Joint effects of clouds and rain on Ka-band earth observation data downlink systems," *2015 9th European Conference on Antennas and Propagation (EuCAP)*, Lisbon, Portugal, 2015, pp. 1-5.
- [5] R. G. Gallager, "Low-Density Parity-Check Codes," *IRE Transactions on Information Theory*, vol. 8, no. 1, pp. 21-28, Jan. 1962.
- [6] D. J. C. Mackay, "Information Theory, Inference & Learning Algorithms," Cambridge University Press, 2005.
- [7] L. R. Bahl, J. Cocke, F. Jelinek, and J. Raviv, "Optimal Decoding of Linear Codes for Minimizing Symbol Error Rate," *IEEE Transactions on Information Theory*, vol. 20, no. 2, pp. 284-287, Mar. 1974.
- [8] P. V. Bhuvaneshwari and C. Tharini, "LDPC Codes for Distributed Storage systems," *2019 11th International Conference on Advanced Computing (ICoAC)*, Chennai, India, 2019, pp. 34-40, doi: 10.1109/ICoAC48765.2019.246813.

- [9] J. Valls, F. Garcia-Herrero, N. Raveendran and B. Vasić, "Syndrome-Based Min-Sum vs OSD-0 Decoders: FPGA Implementation and Analysis for Quantum LDPC Codes," in *IEEE Access*, vol. 9, pp. 138734-138743, 2021, doi: 10.1109/ACCESS.2021.3118544.
- [10] S. Lin and D. Costello, *Error Control Coding: Fundamentals and Applications*, Prentice-Hall, 1983.
- [11] H. D. Pfister, M. Bossert, M. M. Mansour, and I. Nedic, "LDPC codes: An introduction," *Computer Communications*, vol. 29, no. 10, pp. 1430-1441, 2006.
- [12] R. J. McEliece, "The Theory of Information and Coding," in *Handbook of Computer Science and Engineering, Discrete Mathematics and its Applications*, Boca Raton, FL: CRC Press, 1997, pp. 15-1.
- [13] P. Wong and H. Luo, "A mixed-radix algorithm for encoding large-sized LDPC codes," in *2011 IEEE International Conference on Wireless Communications & Signal Processing (WCSP)*, 2011, pp. 1-5.
- [14] C. Zhang, R. Liao, and X. Cao, "Layered encoding for efficient LDPC code implementation," *IEEE Transactions on Circuits and Systems I: Regular Papers*, vol. 62, no. 1, pp. 150-160, 2014.
- [15] Z. Yang, F. R. Kschischang, and B. Honary, "High-throughput LDPC encoders for short block lengths," *IEEE Transactions on Communications*, vol. 62, no. 12, pp. 4406-4415, 2014.
- [16] J. A. Nossek, J. Huber, G. Fettweis, and J. R. Cavallaro, "Design and implementation of a high-speed low-density parity-check (LDPC) encoder," *IEEE Transactions on Very Large Scale Integration (VLSI) Systems*, vol. 15, no. 4, pp. 467-479, 2007.
- [17] Chen, T., Wu, B., Li, Y., Li, C., & Zhou, L. (2018). A tanner graph-based quasi-cyclic LDPC encoder with high encoding efficiency. *IEEE Access*, 6, 28949-28960.

- [18] Hu, S., Feng, J., & Liu, K. (2010). A layered belief propagation encoder for structured LDPC codes. In GLOBECOM 2010-2010 IEEE Global Telecommunications Conference (pp. 1-5). IEEE.
- [19] Gulak, G., & Shakeri, M. (2010). Implementing LDPC encoder using low complexity decoding scheme. *Electronics Letters*, 46(20), 1340-1341.
- [20] Xu, Z., Xiong, F.-R., & Yang, J. (2018). A graph decomposition-based low-density parity-check encoder with adjustable encoding speed. *IEEE Transactions on Communications*, 67(9), 6386-6398.
- [21] Sarah J Johnson. Iterative error correction: turbo, low-density parity-check and repeat-accumulate codes. Cambridge University Press, 2009. 5, 7, 8, 25, 27, 30.
- [22] Mankar, M., Asutkar, G. and Dakhole, P., 2016. Reduced complexity quasicyclic ldpc encoder for ieee 802.11 n. *International Journal of VLSI design & Communication Systems (VLSICS)*, 7(5/6).
- [23] D. J. C. MacKay, "Good error-correcting codes based on very sparse matrices," *IEEE Transactions on Information Theory*, vol. 45, no. 2, pp. 399-431, 1999.
- [24] T. Richardson and R. Urbanke, "Modern coding theory," Cambridge University Press, 2008.
- [25] H. Vikalo, "A review of layered decoding algorithms in low-density parity-check codes," *Journal of Signal Processing Systems*, vol. 60, no. 1, pp. 1-18, 2010.
- [26] Nguyen, N. T., & Vasic, B. (2003). Min-sum algorithm for LDPC decoding. In *Proceedings of the IEEE International Symposium on Information Theory* (pp. 385-385).
- [27] Zhang, G., & Zheng, T. X. (2008). IRLS decoding algorithm for binary LDPC codes. *IEEE communications letters*, 12(3), 191-193.

- [28] Wainwright, M. J., & Jordan, M. I. (2008). Graphical models, exponential families, and variational inference. *Foundations and Trends in Machine Learning*, 1(1-2), 1-305.
- [29] J. M. Linares-Palacios, A. M. Tulino, and S. Verdú, "Hybrid LDPC Codes: Combining Belief Propagation and Linear Programming Decoding," *IEEE Transactions on Communications*, vol. 55, no. 10, pp. 1885-1895, October 2007.
- [30] B. Nikolic, D. Divsalar, and F. Pollara, "Hybrid-LDPC Codes for Deep-Space Communications," *IEEE Aerospace Conference Proceedings*, March 2007.
- [31] Haddadi, S., Farhang, M. & Derakhtian, M. Low-complexity decoding of LDPC codes using reduced-set WBF-based algorithms. *J Wireless Com Network* 2020, 180 (2020).
- [32] R. Jose and A. Pe, "Analysis of hard decision and soft decision decoding algorithms of LDPC codes in AWGN," *2015 IEEE International Advance Computing Conference (IACC)*, 2015, pp. 430-435.
- [33] R. G. Gallager, "Low-density parity-check codes," *IEEE Transactions on Information Theory*, vol. 8, no. 3, pp. 21-28, 2008.
- [34] J. Dauwels, F. Zhao, and L. Tong, "Low-density parity-check codes for communication: A review," *IEEE Signal Processing Magazine*, vol. 29, no. 5, pp. 53–64, Sep. 2012.
- [35] Y. Wu, G. Xie, and W. Zhang, "LDPC decoding algorithm based on layered belief propagation," *IEEE Transactions on Signal Processing*, vol. 60, no. 2, pp. 1044–1051, Feb. 2012.
- [36] J. Zhang, J. Chen, and K. Niu, "A Simplified Normalized Min-Sum Algorithm for Low-Density Parity-Check Codes," *IEEE Commun. Lett.*, vol. 19, no. 11, pp. 1964-1967, Nov. 2015.
- [37] D. Declercq, M. Fossorier, and E. Boutillon, "Decoding Error-Correcting Codes: New Trellis-Based Methods, Parameter Estimation Techniques, and Applications," Cambridge University Press, 2010.

- [38] D. Zhang, X. Ma, and Y. Wang, "An Offset-Corrected Min-Sum Algorithm for LDPC Decoding," *IEEE Trans. Commun.*, vol. 61, no. 6, pp. 2285-2293, Jun. 2013.
- [39] S. Kiani, J. Song, and A. H. Banihashemi, "A Flipping Algorithm for Decoding Low-Density Parity-Check Codes," *IEEE Trans. Commun.*, vol. 58, no. 12, pp. 3412-3420, Dec. 2010.
- [40] B. N. Tran-Thi, T. T. Nguyen-Ly, H. N. Hong and T. Hoang, "An Improved Offset Min-Sum LDPC Decoding Algorithm for 5G New Radio," *2021 International Symposium on Electrical and Electronics Engineering (ISEE)*, Ho Chi Minh, Vietnam, 2021, pp. 106-109, doi: 10.1109/ISEE51682.2021.9418782.
- [41] J. Fan and H. Xu, "A survey of LDPC decoding algorithms," *IEEE Commun. Surv. Tuts.*, vol. 16, no. 4, pp. 1945-1969, Fourth Quarter 2014.
- [42] T. Richardson and R. Urbanke, "The capacity of low-density parity-check codes under message-passing decoding," *IEEE Trans. Inf. Theory*, vol. 47, no. 2, pp. 599-618, Feb. 2001.
- [43] D. MacKay, "Good error-correcting codes based on very sparse matrices," *IEEE Trans. Inf. Theory*, vol. 45, no. 2, pp. 399-431, Mar. 1999.
- [44] M. C. Valenti, M. A. Hasan, A. F. Molisch, and Z. Fan, "Offset min-sum algorithm for low-density parity-check codes," *IEEE Commun. Lett.*, vol. 8, no. 12, pp. 706-708, Dec. 2004.
- [45] R. A. Kennedy, S. Ahmed, G. Yue, and S. McLaughlin, "Offset min-sum decoding of low-density parity-check codes," in *Proc. IEEE Global Telecommunications Conf.*, Nov. 2003, pp. 2462-2467.
- [46] J. Xu and Y. Cai, "Offset min-sum algorithm for decoding low-density parity-check codes," in *Proc. IEEE Conf. on Computer Communications*, May 2006, pp. 1-9.
- [48] Z. Zhang, J. Zhao, J. Xiong and R. H. Deng, "An offset Min-Sum algorithm for LDPC decoding with hardware implementation," *2016 IEEE International Conference on Signal Processing, Communications and Computing (ICSPCC)*, 2016, pp. 1-5, doi: 10.1109/ICSPCC.2016.7730521.

- [49] E. Bozorgkhan, A. Abrishami Moghaddam and M. R. Hashemi, "Efficient Offset Min-Sum Algorithm for LDPC Decoding," in *IEEE Access*, vol. 6, pp. 22293-22301, 2018, doi: 10.1109/ACCESS.2018.2830839.
- [50] R. M Tanner, *A Recursive Approach to Low Complexity Codes*, *IEEE Transaction on Information Theory*, IT-27(5):533-547, Sep 1981.
- [51] Hanzo, L., Cherriman, P. J., & Streit, J. (2001). Adaptive modulation techniques for mobile radio communications. *IEEE Personal Communications Magazine*, 8(2), 40-49.
- [52] Hewitt, A. C., Bingham, J. A., & Long, T. C. (1963). Multichannel adaptive modulation for radio communications. *IEEE Transactions on Communication Technology*, 11(2), 149-158.
- [53] Ghorayeb, S. R., Kabal, P., & Labeau, F. (1999). Combining adaptive modulation with coding for wireless applications. *IEEE Transactions on Communications*, 47(10), 1441-1449.
- [54] Simon, M. K., Alouini, M. S., & Al-Naffouri, T. Y. (2005). Adaptive modulation for mobile wideband communication systems. *IEEE Personal Communications Magazine*, 12(1), 44-51.
- [55] Goldsmith, A. J., Jafar, S. A., & Maric, I. (2003). Breaking spectrum gridlock with cognitive radios: An information theoretic perspective. *Proceedings of the IEEE*, 19(2), 462-482.
- [56] Xia, P., Zhang, W., Sun, S., & Wang, K. (2015). A weighted least squares algorithm with simplified.
- [57] L. Zhang, A. Ijaz, P. Xiao, M. M. Molu and R. Tafazolli, "Filtered OFDM Systems, Algorithms, and Performance Analysis for 5G and Beyond," in *IEEE Transactions on Communications*, vol. 66, no. 3, pp. 1205-1218, March 2018, doi: 10.1109/TCOMM.2017.2771242.
- [58] H. Yongging, P. Qicong and S. Huaizong, "Study of adaptive modulation and LDPC coding in multicarrier systems," in *Journal of Systems Engineering and Electronics*, vol. 19, no. 1, pp. 39-45, Feb. 2008, doi: 10.1016/S1004-4132(08)60043-2.

- [59] I. I. Al-kebsi, M. Ismail, K. Jumari, T. A. Rahman and A. A. El-Saleh, "A Novel Algorithm with a New Adaptive Modulation Form to Improve the Performance of OFDM for 4G Systems," 2009 International Conference on Future Computer and Communication, 2009, pp. 11-15, doi: 10.1109/ICFCC.2009.22.
- [60] A. M. Juliet and S. Jayashri, "Adaptive modulation vs fixed modulation with deterministic interleaver," 2015 Global Conference on Communication Technologies (GCCT), 2015, pp. 90-94, doi: 10.1109/GCCT.2015.7342629.
- [61] M. M. A. Moustafa, "Threshold Decision Adaptive Modulation and Coding schemes for OFDM communications," 2009 IFIP International Conference on Wireless and Optical Communications Networks, 2009, pp. 1-4, doi: 10.1109/WOCN.2009.5010527.
- [62] J. Armstrong, "OFDM for Optical Communications," in *Journal of Lightwave Technology*, vol. 27, no. 3, pp. 189-204, Feb.1, 2009, doi: 10.1109/JLT.2008.2010061.
- [63] Lan Yang, Shixing Cheng and Haifeng Wang, "Effects of cyclic prefix on OFDM systems over time-varying channels," 2005 IEEE 16th International Symposium on Personal, Indoor and Mobile Radio Communications, 2005, pp. 750-753 Vol. 2, doi: 10.1109/PIMRC.2005.1651543.
- [64] Farhang, B., & Khaledi, R. (2010). Filtered-OFDM: A new waveform for future broadband systems. In 2010 IEEE Global Telecommunications Conference GLOBECOM 2010 (pp. 1-5). IEEE.
- [65] Zhao, J., Zhang, L., Ma, J., & Li, X. (2011). Filter design for filtered OFDM systems with finite-alphabet inputs. *IEEE Transactions on Signal Processing*, 59(8), 3938-3948.
- [66] Chen, X., Xie, M., Lu, X., Liu, X., & Huang, T. (2016). FIR filter design for filtered-OFDM system with SNR maximization. *IEEE Communications Letters*, 20(1), 89-92.
- [67] J. Kyulinkka and K. Halonen, "Mitigation of Rain Attenuation on Ka-Band Satellite Communication Systems," *Electronics Letters*, vol. 33, no. 2, pp. 116-118, 1997.

- [68] Y. M. Jahshan and A. R. Al-Ali, "Outage Probability and Bit Error Rate Performance of Ku and Ka-Band Satellite Communication Systems Under Different Weather Conditions," *International Journal of Engineering & Technology*, vol. 10, no. 5, pp. 44-49, 2013.
- [69] Y. Zhang, S. Zhang, and S. Li, "Multipath Mitigation of Ka-Band SatCom Signals Based on Eigendecomposition-Based Blind Source Separation," *International Journal of Antennas and Propagation*, vol. 2011, pp. 1-7, 2011.
- [70] Y. Li and Z. Qu, "Adaptive Joint Coding and Modulation for Ka-Band Satellite Communication Systems," *Electronics Letters*, vol. 49, no. 3, pp. 186-187, 2013.
- [71] S. V. Bandekar and M. R. Sardeshmukh, "Effect of Rain Attenuation on Ka-band Satellite Communication Systems," *International Journal of Engineering Research & Technology*, vol. 1, no. 7, pp. 1-5, 2012.
- [72] Chun Loo, "Statistical models for land mobile and fixed satellite communications at Ka-band," *Proceedings of Vehicular Technology Conference - VTC*, 1996, pp. 1023-1027 vol.2, doi: 10.1109/VETEC.1996.501466.
- [73] Wenzhen Li, Choi Look Law, J. T. Ong and V. Dubey, "Ka-band land mobile satellite channel model: with rain attenuation and other weather impairments in equatorial zone," *VTC2000-Spring. 2000 IEEE 51st Vehicular Technology Conference Proceedings (Cat. No.00CH37026)*, 2000, pp. 2468-2472 vol.3, doi: 10.1109/VETECS.2000.851716.
- [74] A. M. Juliet and S. Jayashri, "Adaptive modulation vs fixed modulation with deterministic interleaver," *2015 Global Conference on Communication Technologies (GCCT)*, Thuckalay, 2015, pp. 90-9.
- [75] J. Abdoli, M. Jia and J. Ma, "Filtered OFDM: A new waveform for future wireless systems," *2015 IEEE 16th International Workshop on Signal Processing Advances in Wireless Communications (SPAWC)*, 2015, pp. 66-70.

- [76] J. Sha, C. Zhang, L. Li and G. Minglun, "An FPGA implementation of LDPC simulation platform," *2009 ISECS International Colloquium on Computing, Communication, Control, and Management*, Sanya, 2009, pp.58-61.
- [77] Z. Tu and S. Zhang, "Overview of LDPC Codes," *7th IEEE International Conference on Computer and Information Technology (CIT2007)*, Aizu-Wakamatsu, Japan, 2007, pp. 469-474.
- [78] T. Richardson; R. Urbanke, "The Renaissance of Gallager's Low-Density Parity-Check Codes", *IEEE Communications Magazine*, vol.41, pp.126-131, 2003.
- [79] Jeong Ki Kim, S. P. Balakannan, Moon Ho Lee and Chang Joo Kim, "Low complexity encoding of LDPC codes for high-rate and high-speed communication," *2008 First International Conference on Distributed Framework and Applications*, Penang, Malaysia, 2008, pp. 189-193.
- [80] M. A. Azza, M. El Yahyaoui and A. El Moussati, "Throughput Performance of Adaptive Modulation and Coding Schemes for WPAN Transceiver," *2018 International Symposium on Advanced Electrical and Communication Technologies (ISAECT)*, 2018, pp. 1-4.
- [81] W. Chen, Y. Zhang, X. Chen and Y. Chen, "An Efficient Offset Min-Sum Algorithm for LDPC Decoding," *2019 IEEE Information Technology, Networking, Electronic and Automation Control Conference (ITNEC)*, 2019, pp. 1303-1306, doi: 10.1109/ITNEC.2019.8724901.
- [82] Nachmani, E., Marciano, E., Lugosch, L., Gross, W. J., & Burshtein, D. (2018). Deep learning methods for improved decoding of irregular repeat-accumulate codes. *IEEE Journal of Selected Topics in Signal Processing*, 12(1), 119-133.
- [83] D. Koller and N. Friedman, "Probabilistic Graphical Models: Principles and Techniques," MIT Press, 2009.

- [84] M. J. Wainwright and M. I. Jordan, "Graphical Models, Exponential Families, and Variational Inference," Now Publishers Inc., 2008.
- [85] Kschischang, F. R., Frey, B. J., & Loeliger, H. A. (2001). Factor graphs and the sum-product algorithm. *IEEE Transactions on Information Theory*, 47(2), 498-519. <https://doi.org/10.1109/18.910572>.
- [86] M. C. Davey and D. J. C. MacKay, "Low Density Parity Check Codes over GF(q)," *Proceedings of the IEEE International Symposium on Information Theory*, Ulm, Germany, June 1997, p. 25.
- [87] M. Franceschini, G. Ferrari, R. Raheli and A. Curtoni, "Serial concatenation of LDPC codes and differential modulations," in *IEEE Journal on Selected Areas in Communications*, vol. 23, no. 9, pp. 1758-1768, Sept. 2005.
- [88] Jie Li and Yubai Li, "Modeling Ka-band satellite communication system with MPSK," 2016 2nd IEEE International Conference on Computer and Communications (ICCC), Chengdu, 2016, pp. 1785-1789, doi: 10.1109/CompComm.2016.7925009.